

THE ESTIMATION OF THE SPATIAL VARIABILITY OF THE FLOW
PARAMETERS USING HYDRAULIC TOMOGRAPHY

by

Mehmet Taner Demir

B.S. in Electrical and Electronics Engineering, Boğaziçi University, 2010

Submitted to the Institute of Environmental Sciences in partial fulfillment of

the requirements for the degree of

Master of Science

in

Environmental Technology

Boğaziçi University

2013

ACKNOWLEDGEMENTS

First of all, I would like to express my gratitude to my supervisor Prof. Dr. Nadim Copty for his sincere support and encouragement through the thesis process. I am deeply thankful to him for his guidance since the day he accepted to be my thesis advisor. Without his intellectual, analytical and motivational contribution, this thesis would not have been possible.

I am also thankful to the jury members of my thesis; Assistant Prof. Dr. Başak Güven and Associate Prof. Dr. Melek Kazezyılmaz Alhan for their valuable comments. Moreover, I am indebted to my course advisor, Prof. Dr. Ayşen Erdinçler, for her excellent guidance and help throughout my master's degree education.

In addition, I owe special thanks to my dearest friends; Şebnem, Didem, Hacer, Güher, Ahmet, Mesut, Samet, İstem, Ece, Şeyda, Ezgi, Esra, Ceren, Tuğba, Gülçin, Raselin, Çağan, İrem and Melih for all their love and support. No word can express how grateful I am to them and how much they mean to me.

I am also grateful to my colleagues, Duygu Can, Ece Ersöz, Cemre Birben and Serkan Kaptan for their generous help and friendship. During the thesis writing process, their suggestions were very valuable and appreciated. I consider myself lucky for being a friend of them.

Finally, I would like to express my deepest gratitude to my family. My mother Fethiye Demir and my father İsmail Demir always supported my decisions and they always wanted the best for me. I would have never found my way without their unconditional love, encouragement, understanding and belief in me.

This research was supported by Boğaziçi University Research Fund, with Project No: 6722, which is very much appreciated.

ABSTRACT

Natural geologic systems are heterogeneous with complex patterns of spatial variability and this heterogeneity strongly influences groundwater flow and contaminant transport. Therefore, the estimation of the spatial variability of subsurface flow parameters is essential for the modeling and prediction of groundwater flow and contaminant transport.

Pumping tests are often used for the estimation of flow parameters. However, the interpretation of these tests is routinely performed using conventional methods that assume the parameters are uniform which is in contradiction with most real systems. The main objective of this thesis is to combine a recently developed pumping test interpretation technique, referred to as the Continuous Derivation method, with data obtained from hydraulic tomography. Hydraulic tomography is a novel field data acquisition technique that involves the sequential pumping from a number of wells and observing the groundwater drawdown in adjacent wells as a function of time. Particularly, the goal was to extend the method to the estimation of the statistical spatial structure of the transmissivity using hydraulic tomography data. In geostatistics, the statistical spatial structure of a parameter refers to the pattern of how this parameter varies in space. The emphasis was on estimating how the transmissivity varies with distance from the pumping well and then use that information to estimate the statistical parameters, namely the integral scale and variance.

Synthetic pumping tests were used to evaluate the performance of the pumping test interpretation procedure. Heterogeneous transmissivity fields were first generated and then used to simulate transient drawdown data. The drawdown data and their time derivatives were subsequently used to estimate the flow parameters by applying the Continuous Derivation method. Single-well pumping test data as well as hydraulic tomography data derived from multiple wells were used in the interpretation method. After that, two approaches, a weighted least-squares approach and a Bayesian approach were considered

for the estimation of the statistical parameters of the heterogeneous transmissivity field (integral scale and variance).

The results of this study indicate that some information about the spatial structure of the transmissivity can be inferred from pumping tests. The estimation of the variance and the integral scale is however challenging in part due to the lack of ergodicity when the number of pumping test is low. The Bayesian approach was found to be somewhat superior because of its ability to account for parametric uncertainty by formulating the parameter estimation problem in a probabilistic framework.

ÖZET

Doğal jeolojik sistemler heterojendirler. Bu heterojenlik yeraltı suyu akışını ve kirliliğin taşınımını çok kuvvetli bir şekilde etkiler. Bu yüzden, yeraltı sularının akış parametrelerini hesaplamak, yeraltı suyu akışını ve kirliliğin taşınımını modellemek ve hesaplamak açısından oldukça önemli ve gereklidir.

Akış parametrelerini hesaplamak için sıklıkla pompaj testleri kullanılır. Fakat bu testlerin analizi genel olarak, gerçek sistemlerin aksine, parametrelerin tek tip olduğunu varsayan geleneksel metodlarla gerçekleştirilmektedir. Bu tezin ana hedefi yakın zamanda geliştirilmiş yeni bir pompaj testi yorumlama tekniği olan Devamlı Derivasyon metodunu hidrolojik tomografiden elde edilen data ile birleştirmektir. Hidrolojik tomografi sahadan data elde etmek için kullanılan yeni tekniklerden biridir ve birden fazla pompaj testinin zamana bağlı yeraltı su seviyesi alçalma datalarının ardışık olarak elde edilmesini sağlar. Bu çalışmada özellikle hedeflenen şey, yukarıda bahsedilen metodu geliştirerek, geçirgenliğin istatistiksel uzamsal yapısını hidrolojik tomografi datalarını kullanarak hesaplamaktır. Jeostatistikte, parametrelerin istatistiksel uzamsal yapısı, onların konuma bağlı olarak nasıl değiştiğini gösterir. Bu çalışmada yapılmak istenen şey; geçirgenliğin pompaj kuyularından uzaklaştıkça nasıl değiştiğini hesaplamak ve de bu değişkenlik dadasını, istatistiksel parametreler olan varyans ve integral ölçeğini hesaplamak için kullanmaktır.

Bu çalışmada, pompaj testi yorumlama yönteminin performansını değerlendirmek için sentetik pompaj testleri kullanıldı. Önce heterojen geçirgenlik alanları oluşturuldu ve ardından bu alanlar su seviyesinin kısa süreli alçalma dadasını elde etmek için kullanıldı. Akış parametrelerini hesaplamak için, Devamlı Derivasyon metodu uygulanarak su seviyesinin kısa süreli alçalma dadası ve zamana göre türevi elde edildi. Pompaj teslerini yorumlamak için kullanılan bu datalar hem tek kuyuya uygulanan pompaj testi yöntemi ile hem de birden fazla kuyuyu içeren hidrolik tomografi yöntemi ile elde edildi. Sonrasında, heterojen geçirgenlik alanlarının istatistiksel parametrelerin hesaplanması için iki yaklaşım kullanıldı: Bayezyen yaklaşım ve ağırlıklı en küçük kareler yaklaşımı.

Bu çalışmanın sonuçları pompaj testleri sayesinde geçirgenliğin uzamsal yapısı hakkında bazı bilgiler elde edebileceğimizi gösterdi. Fakat, pompaj test sayısının azlığının sebep olduğu ergodik eksiklik, varyans ve integral ölçüğünün hesaplanmasını zorlaştırıyor. Bayezyen yaklaşımın, ağırlıklı en küçük kareler yaklaşımına göre daha iyi sonuçlar verdiğini söylemek mümkün. Bu durum Bayezyen yöntemin parametrelerin hesaplanması için kullandığı olasılıksal yaklaşım ile açıklanabilir.

TABLE OF CONTENTS

ACKNOWLEDGEMENTS.....	iii
ABSTRACT.....	iv
ÖZET	vi
TABLE OF CONTENTS.....	viii
LIST OF FIGURES	x
LIST OF TABLES	xiii
LIST OF SYMBOLS/ABBREVIATIONS.....	xiv
1. INTRODUCTION	1
2. RESEARCH OBJECTIVES	7
3. LITERATURE REVIEW.....	9
3.1. Pumping Tests in Homogeneous Media	9
3.2. Stochastic Modeling Approach for Groundwater Problems	11
3.2.1. Geostatistical Approach	11
3.2.2. Stochastically Interpretation of Pumping Test Data	12
3.3. Hydraulic Tomography	14
4. METHODOLOGY.....	17
4.1. Conventional Methods for Confined Aquifers.....	17
4.1.1. Theis Method	18
4.1.2. Cooper-Jacob Method.....	20
4.2. Novel Methods for Confined Aquifers	22
4.2.1. Continuous Derivation Method	23
4.3. Estimation of Integral Scale and Variance.....	26
4.3.1. Weighted Least-Squares Approach	27
4.3.2. Bayesian Approach	28
4.4. Numerical Simulation	30
5. RESULTS AND DISCUSSION	34
5.1. Generation of Transmissivity Fields	34
5.2. Hydraulic Tomography Results	37
5.3 The Estimation of Variance and Integral Scale.....	46

5.3.1 Weighted Least-Squares Method	47
5.3.1 Bayesian Method.....	58
6. CONCLUSIONS AND RECOMMENDATIONS	69
REFERENCES	72
APPENDIX A: COMPUTER CODE FOR THE APPLICATION OF CONTINUOUS DERIVATION METHOD.....	78
APPENDIX B: COMPUTER CODE FOR THE ESTIMATION OF STATISTICAL PARAMETERS	86

LIST OF FIGURES

Figure 2.1. Heterogeneous confined aquifer (Kruseman and de Ridder, 1991).	8
Figure 3.1. Pumping test (Kruseman and de Ridder, 1991).	10
Figure 3.2. Multiple wells located on a synthetically-generated transmissivity field for use with hydraulic tomography.	15
Figure 4.1. Drawdown change in a confined aquifer (Fetter, 2001).	18
Figure 4.2. Theis curve (Batu, 1998).	20
Figure 4.3. An example for Cooper-Jacob straight-line fitting (Batu, 1998).	22
Figure 4.4. The plot of γc as a function of $1/u$	24
Figure 4.5. Theoretical transmissivity curves consisting of the geometric mean of the transmissivity as a function of radial distance for different values of variance and integral scale.	26
Figure 4.6. The flow chart showing the main steps of this study.	33
Figure 5.1. Randomly generated $\ln T$ fields with same mean, variance and integral scale values ($m_y=0$; $\sigma^2=1$; $I=8$).	35
Figure 5.2. Effect of variance on the generated transmissivity fields with $\sigma^2=1, 2$ respectively.	36
Figure 5.3. Effect of integral scale on the generated transmissivity fields with $I=1, 2$ respectively.	37
Figure 5.4. Location of wells (randomly selected) for hydraulic tomography superimposed over one of the randomly-generated $\ln T$ fields.	38
Figure 5.5. Drawdown results obtained from hydraulic tomography for d) Well-4, e) Well- 5 and f) Well-6.	40
Figure 5.6. Transmissivity curves at each well for a) pumping test-1, b) pumping test-2, c) pumping test-3.	41
Figure 5.7. Transmissivity curves at each well for d) pimping test-4, e) pimping test-5, f) pumping test-6.	42
Figure 5.8. Estimated transmissivity using the continuous derivative method along with the geometric mean of the transmissivity as a function of radial distance from a) Well 1, b) Well 2, c) Well 3.	43

Figure 5.9. Estimated transmissivity using the continuous derivative method along with the geometric mean of the transmissivity as a function of radial distance from d) Well 4, e) Well 5, f) Well 6.	44
Figure 5.10. Estimation of statistical parameters, the variance and the integral scale, for the estimated transmissivity as a function of radial distance from the well.	46
Figure 5.11. Histogram of (a) estimated variance and (b) estimated integral scale using weighted least-squares assuming n=1 pumping test is available for Set 1 transmissivity fields ($\sigma^2=1$ and $I=8$).....	49
Figure 5.12. Histogram of (a) estimated variance and (b) estimated integral scale using weighted least-squares assuming n=5 pumping test is available for Set 1 transmissivity fields ($\sigma^2=1$ and $I=8$).....	50
Figure 5.13. Histogram of (a) estimated variance and (b) estimated integral scale using weighted least-squares assuming n=10 pumping test is available for Set 1 transmissivity fields ($\sigma^2=1$ and $I=8$).....	51
Figure 5.14. Histogram of (a) estimated variance and (b) estimated integral scale using weighted least-squares assuming n=1 pumping test is available for Set 2 transmissivity fields ($\sigma^2=2$ and $I=8$).....	52
Figure 5.15. Histogram of (a) estimated variance and (b) estimated integral scale using weighted least-squares assuming n=5 pumping test is available for Set 2 transmissivity fields ($\sigma^2=2$ and $I=8$).....	53
Figure 5.16. Histogram of (a) estimated variance and (b) estimated integral scale using weighted least-squares assuming n=10 pumping test is available for Set 2 transmissivity fields ($\sigma^2=2$ and $I=8$).....	54
Figure 5.17. Histogram of (a) estimated variance and (b) estimated integral scale using weighted least-squares assuming n=1 pumping test is available for Set 3 transmissivity fields ($\sigma^2=1$ and $I=24$).....	55
Figure 5.18. Histogram of (a) estimated variance and (b) estimated integral scale using weighted least-squares assuming n=5 pumping test is available for Set 3 transmissivity fields ($\sigma^2=1$ and $I=24$).....	56
Figure 5.19. Histogram of (a) estimated variance and (b) estimated integral scale using weighted least-squares assuming n=10 pumping test is available for Set 3 transmissivity fields ($\sigma^2=1$ and $I=24$).....	57

Figure 5.20. Histogram of (a) estimated variance and (b) estimated integral scale using Bayesian method assuming n=1 pumping test is available for Set 1 transmissivity fields ($\sigma^2=1$ and $I=8$).	60
Figure 5.21. Histogram of (a) estimated variance and (b) estimated integral scale using Bayesian method assuming n=5 pumping test is available for Set 1 transmissivity fields ($\sigma^2=1$ and $I=8$).	61
Figure 5.22. Histogram of (a) estimated variance and (b) estimated integral scale using Bayesian method assuming n=10 pumping test is available for Set 1 transmissivity fields ($\sigma^2=1$ and $I=8$).	62
Figure 5.23. Histogram of (a) estimated variance and (b) estimated integral scale using Bayesian method assuming n=1 pumping test is available for Set 2 transmissivity fields ($\sigma^2=2$ and $I=8$).	63
Figure 5.24. Histogram of (a) estimated variance and (b) estimated integral scale using Bayesian method assuming n=5 pumping test is available for Set 2 transmissivity fields ($\sigma^2=2$ and $I=8$).	64
Figure 5.25. Histogram of (a) estimated variance and (b) estimated integral scale using Bayesian method assuming n=10 pumping test is available for Set 2 transmissivity fields ($\sigma^2=2$ and $I=8$).	65
Figure 5.26. Histogram of (a) estimated variance and (b) estimated integral scale using Bayesian method assuming n=1 pumping test is available for Set 3 transmissivity fields ($\sigma^2=1$ and $I=24$).	66
Figure 5.27. Histogram of (a) estimated variance and (b) estimated integral scale using Bayesian method assuming n=5 pumping test is available for Set 3 transmissivity fields ($\sigma^2=1$ and $I=24$).	67
Figure 5.28. Histogram of (a) estimated variance and (b) estimated integral scale using Bayesian method assuming n=10 pumping test is available for Set 3 transmissivity fields ($\sigma^2=1$ and $I=24$).	68

LIST OF TABLES

Table 1.1. Estimation of global water distribution	2
--	---

LIST OF SYMBOLS/ABBREVIATIONS

Symbol	Explanation	Units used
h	Hydraulic Head	
h_o	Initial Hydraulic Head	(m)
I	Integral Scale	(unitless)
K	Hydraulic Conductivity	(m/s)
m_y	Mean of Natural Log of Transmissivity	(unitless)
n	Number of Pumping Tests	(unitless)
Q	Constant Discharge Rate	(m ³ /day)
S	Storativity	(unitless)
S_i	Time-dependent Storativity	(unitless)
S_s	Specific Storage Coefficient	(1/m)
s	Transient Drawdown	(m)
s'	First Derivative of Transient Drawdown	(m)
T	Transmissivity	(m ² /s)
T_e	Estimated Transmissivity	(m ² /s)
T_{geo}	Geometric Mean of Transmissivity Field	(m ² /s)
T_i	Time-dependent Transmissivity	(m ² /s)
T_{th}	Theoretical Transmissivity	(m ² /s)
u	Dimensionless time factor	(unitless)
Y	Natural Log-transform of Transmissivity	(unitless)

CD	Continuous Derivation Method	
PDF	Probability Density Function	
RSV	Random Spatial Variable	
$\gamma(h)$	Exponential Semi-variogram	(unitless)
γ_c	Drawdown-First derivative Ratio	(unitless)
σ^2	Variance	(unitless)

1. INTRODUCTION

The hydrologic cycle is the endless circulation of water within the different compartments of the Earth system, namely the oceans, lands and atmosphere. The hydrologic cycle has a remarkable influence on a large number of fields such as agriculture, geography, forestry, global energy exchange and water supply. Groundwater, which is defined as the water beneath the land surface, is one of the major components of the hydrologic cycle. It is stored within geologic formations referred to as aquifers which allow significant groundwater flow, aquitards which tend to retard the flow of water and which act as storage reservoirs for aquifers, and aquicludes which are impermeable layers of rock or soil that prevent the flow of groundwater through them (Walton, 1970; Freeze and Cherry, 1979).

Groundwater constitutes about 1.7% of the total global water distribution, with the oceans comprising 96.5% and ice caps and glaciers making up about 1.76% (Table 1.1). Water in rivers and lakes which are often used for domestic and industrial water use make up no more than 0.013 %. The importance of groundwater can be seen when we examine the global distribution of freshwater, with groundwater making up more than 30% of this resource. Recognizing that about 69% of all fresh water is in the form of glaciers, permanent snow or ice caps, the significance of groundwater resources becomes further evident (Shiklomanov, 1993).

Groundwater is an essential source of water for more than two billion people worldwide (Kemper, 2004). The significance of the role of groundwater is that domestic and municipal use, industry, and agriculture are inevitably dependent on groundwater as a water supply. For example, a large amount of the world's irrigation is enabled with groundwater. The groundwater supplied for irrigation helps the crops to grow under unattractive climate conditions. Moreover groundwater provides large volumes of water that is combined with surface water for municipal and industrial water distribution

networks. As a domestic supply, groundwater is very crucial for many homes which are far from urban water supplement channels (Pinder and Celia, 2006).

Table 1.1. Estimation of global water distribution (Shiklomanov, 1993).

Water source	Water volume, in cubic miles	Water volume, in cubic kilometers	Percent of freshwater	Percent of total water
Oceans, Seas, & Bays	321,000,000	1,338,000,000	--	96.5
Ice caps, Glaciers, & Permanent Snow	5,773,000	24,064,000	68.6	1.74
Ground water	5,614,000	23,400,000	--	1.7
Fresh	2,526,000	10,530,000	30.1	0.76
Saline	3,088,000	12,870,000	--	0.93
Soil Moisture	3,959	16,500	0.05	0.001
Ground Ice & Permafrost	71,970	300,000	0.86	0.022
Lakes	42,320	176,400	--	0.013
Fresh	21,830	91,000	0.26	0.007
Saline	20,490	85,400	--	0.007
Atmosphere	3,095	12,900	0.04	0.001
Swamp Water	2,752	11,470	0.03	0.0008
Rivers	509	2,120	0.006	0.0002
Biological Water	269	1,120	0.003	0.0001

Population growth, industrial and agricultural developments have, however, often become a threat to groundwater resources. As one of the most important freshwater resource potentials of the world, groundwater has to be protected from the increasing risk of contamination. Although it constitutes a large percentage of the readily available water, its rate of renewal is finite and limited. Furthermore, unrestrained disposal of urban, industrial and agricultural wastes are resulting in the degradation of aquifers worldwide (Freeze and Cherry, 1979). The uncontrolled overexploitation of groundwater is also threatening large volumes of this resource.

From the above considerations, it is obvious that the sustainable use and management of groundwater is of great importance since groundwater has an essential role as one of the most valuable natural resources.

The hydrogeologic characteristics of subsurface systems influence the quality and the quantity of available groundwater. More specifically, water flow and its storage in subsurface reservoirs are affected by the characteristics of the geologic formations whose hydrologic properties which include the key parameters: hydraulic conductivity or transmissivity and storativity (Batu, 1998). The hydraulic conductivity and transmissivity refer to the rate of water transmission through the soil while the storativity relates to the water storage within the porous medium which is related to the porosity of the porous media and the media compressibility (Freeze and Cherry, 1979).

Numerous site investigations have shown that hydrogeologic parameters have large spatial variability due to the heterogeneous structure of the subsurface systems. These spatial variations play an important role on the infiltration, transport and storage of the groundwater. The spatial variability of the flow parameters also influences the spread of contaminants (Dagan, 1989; Gelhar 2003). In order to evaluate groundwater resources, to predict subsurface contaminant transport and to implement, where needed, groundwater remediation activities, the spatial variability of the flow parameters, most notably the hydraulic conductivity (K), has to be estimated accurately (Rubin, 2005). In other words, the accurate estimation of the flow parameters is an essential step for the modeling and prediction of groundwater flow and contaminant transport.

The most common method for the determination of aquifer hydraulic characteristics is pumping tests (Domenico and Schwartz, 1998). In a pumping test, groundwater is extracted from the ground at a pumping well and the drawdown level -or the drop in hydraulic head- as a function of time is measured at different locations. The data gathered from such tests are analyzed and modeled in order to estimate the hydraulic parameters, such as transmissivity, storativity and leakage factor, that are subsequently used in any modeling effort (Batu, 1998). The interpretation of pumping test practices were first formalized in the studies of Theis (1935) and Cooper and Jacob (1946) for confined aquifers, and Hantush and Jacob (1955) for leaky aquifers. These classical methods,

however, assume the flow parameters as uniformly distributed in space. In contrast to the assumption of the homogeneity of the subsurface system, observations made in numerous fields, show that hydraulic parameters are almost always characterized by complex spatial variations (Dagan, 1989; Gelhar 2003; Rubin 2003). Further discussion of existing pumping test interpretation techniques is given in Section 4.

In order to better characterize real aquifer systems that exhibit large heterogeneities, hydraulic tomography, a novel field data acquisition technique, has been proposed recently. It involves sequential pumping at one of a series of wells and observing the drawdown due to pumping at adjacent wells (Gottlieb and Dietrich, 1995; Butler et al., 1999; Yeh and Liu, 2000; Bohling et al., 2002). The interpretation of the drawdown data from hydraulic tomography for the estimation of the spatial variability of the flow parameters has been mostly performed using formal inverse procedures which are numerically demanding because of the non-uniqueness and instability of the groundwater inverse problems.

Alternatively, due to the limitation of primary hydrological data from pumping tests some researchers have considered the use of secondary data related to the spatial distribution of flow parameters; such as tracer test data (Bellin and Rubin, 2004; Huang et al., 2004) and geophysical data (Rubin and Hubbard, 2005; Slater, 2007). Thus, secondary information has been used in order to alleviate the problems and limitations resulting from the lack of the direct field data about the spatial structure of subsurface formations.

Furthermore, the heterogeneity of the flow parameters leads to a large level of uncertainty and nonuniqueness problems in the definition of the parameters. Thus, recent works on spatial variability have considered the use of stochastic approaches for groundwater problems. By using stochastic formulations, data are defined in terms of probability distributions rather than single deterministic values.

One of the most commonly methods of stochastic approach is geostatistics (Yeh et al., 1995; Kitanidis, 1997; Sanchez-Vila, 1999; Bohling, 2005). Geostatistics is the application of statistical methods to the earth sciences including groundwater flow and contaminant transport. Within a geostatistical framework, flow parameters, such as the

hydraulic conductivity, are defined as a random spatial variable (RSV) which can be expressed in terms of few statistical parameters, namely the spatial mean, variance and integral scale (Renard, 2007). The stochastic formulation of the groundwater problem is described in more details in Section 3.2.2 of this thesis.

The modeling of groundwater flow and contaminant transport has evolved in recent decades into an essential tool for the analysis of subsurface flow system. However, the simulation of groundwater flow and contaminant transport requires the definition of the flow parameters over the entire flow domain. Because flow and transport are strongly influenced by the heterogeneity of the subsurface system, incorporating the spatial variability of the flow parameters is essential for the accurate prediction of water and contaminant transport (Kumar, 2002).

In groundwater modeling the governing groundwater flow equations are generally solved analytically or numerically. While the analytical modeling solves the equations continuously in space and time; they are generally possible for more simplified problems. For more complex real problems, numerical solution are often needed to solve the partial differential equations discretely in space and time domains by approximating the equations numerically (Kumar, 2002). The finite-difference and finite-elements methods are among the most used numerical approximation methods (McDonald and Harbaugh, 1988). A groundwater flow simulator, MODFLOW, which is perhaps the most commonly used groundwater flow simulator and which will be used in this study to simulate pumping tests, employs the finite-difference method in order to model the groundwater flow (Harbaugh et al., 2000). The method of finite difference estimates derivatives appearing in the governing differential equation in terms of differences, resulting in a system of algebraic equations which are solved in time or space for the dependent variables such as hydraulic head or concentration. Irrespective of the method used to solve the governing groundwater equations, defining the flow parameters, such as hydraulic conductivity, over the entire flow domain remains a critical step for the accurate prediction for groundwater flow and contaminant transport.

The rest of this thesis is organized as follows: Section 2 describes the main objectives of the study. Section 3 presents a review of the related literature. Section 4

describes the developed methodology for the interpretation of pumping test data from heterogeneous confined aquifers. It also includes the methods used for the generation of synthetic pumping test data which are used to test the developed method. Section 5 presents the numerical results obtained in this Study. Finally, Section 6 provides a summary of this effort with final recommendations and possible avenues for future research.

2. RESEARCH OBJECTIVES

The main objective of this study is to combine a recently developed pumping test interpretation technique with data obtained from hydraulic tomography. Specifically, the objective is to develop a technique for the estimation of the statistical spatial structure of the transmissivity from hydraulic tomography data. The method relies on the pumping test interpretation procedure of Coptý et al. (2011) which uses the time-drawdown data and its time derivative at each observation well to estimate the spatially averaged transmissivity as a function of radial distance from the pumping well. Most of the novel interpretation techniques have relied on data from a single well. The main novelty of this study is that it uses the data from multiple wells that are obtained from hydraulic tomography by jointly taking the estimated parameters and how they vary with distance from the pumping well. Furthermore, the method goes beyond previous studies by attempting to estimate the transmissivity at the well as well as statistical parameters that describe its spatial variability, namely the integral scale and variance.

It is important to note that given the complexity and nonuniqueness of the parameter estimation problem, to estimate the actual transmissivity values over the entire domain from the pumping tests is impossible (Dagan, 1989). The goal of this method is to infer as much information about the spatial variability of transmissivity. In practice, this means attempting to estimate transmissivity mean as well as the statistical parameters describing the distribution of the transmissivity.

The spatial structure will be interpreted for heterogeneous confined aquifers which are bounded from the top and bottom by impervious layers that do not allow water to flow vertically into the aquifer (Figure 2.1). The aquifer domains are assumed as laterally unbounded and the flow is assumed as two dimensional with fully penetrating wells of infinitesimal well radius.

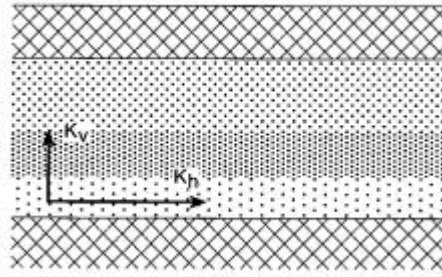


Figure 2.1. Heterogeneous confined aquifer (Kruseman and de Ridder, 1991).

The specific objectives of this study will be to:

- Evaluate pumping test interpretation methods using single-well pumping test data from heterogeneous aquifers.
- Expand the method to cases when data from multiple wells are available (hydraulic tomography).
- Develop and test different procedures for the estimation of the statistical parameters of the heterogeneous transmissivity field (integral scale and variance).
- Assess the potential of using pumping test data to infer information about the spatial variability of the transmissivity.

3. LITERATURE REVIEW

3.1. Pumping Tests in Homogeneous Media

The estimation of the flow parameters is a prerequisite for the modeling and prediction of groundwater flow and contaminant transport (Dagan, 1989). The two primary parameters that control the flow of groundwater are the transmissivity (T) and the storativity parameters (S). Transmissivity (or hydraulic conductivity for three-dimensional flow) can be defined as the ability for the water to move through the soil whereas the storativity is defined as the amount of water which can be released from storage due to a change in head and is related to the porosity of the porous media and its compressibility (Freeze and Cherry, 1979). The governing partial differential equation describing two dimensional flow through an aquifer is:

$$\frac{\partial^2 h}{\partial x^2} + \frac{\partial^2 h}{\partial y^2} = \frac{S}{T} \frac{\partial h}{\partial t} \quad (3.1)$$

where h is the hydraulic head, S and T are the storativity and transmissivity respectively, x and y are the spatial coordinates and t is time. The above equation assumes that the storativity and transmissivity are spatially uniform over the entire flow region.

One of the most commonly used methods in the field for the estimation of the flow parameters is pumping tests (Domenico and Schwartz, 1998). Pumping tests are conducted by extracting groundwater from a pumping well and by measuring the drawdown level -or drop in hydraulic head- as a function of time at one or more observation wells (Figure 3.1).

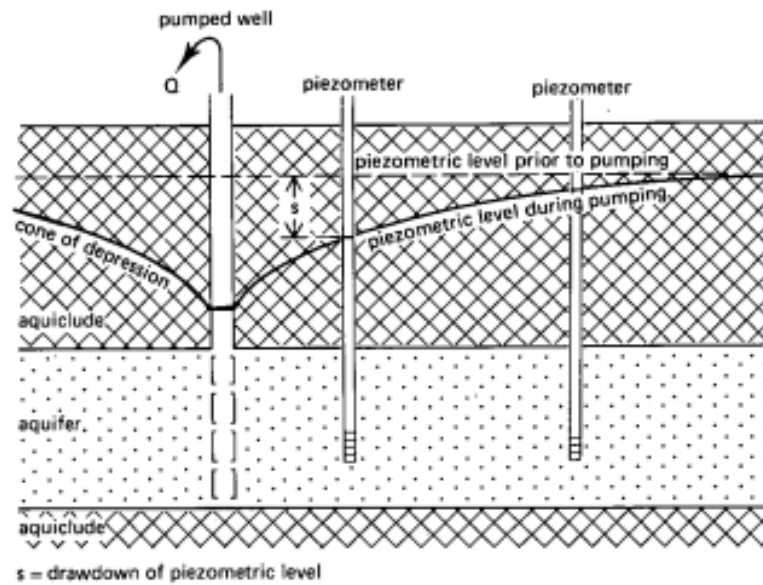


Figure 3.1. Pumping test (Kruseman and de Ridder, 1991).

The interpretation and analysis of pumping tests are critical steps for obtaining information about the subsurface systems. By analyzing and modeling drawdown data gathered from pumping tests, hydraulic parameters, such as transmissivity, storativity and leakage factor which is present for leaky aquifers, are estimated and subsequently can be used in any modeling effort (Batu, 1998).

Commonly employed pumping test analysis techniques produce average values for the flow parameters. These conventional methods treat the subsurface as a homogeneous unit by assuming the flow parameters to be uniformly distributed in space. That is, the transmissivity (or hydraulic conductivity) values are assumed as single and homogeneous values. Most of these classical methods are based on the Theis Method (Theis, 1935). This method predicts the drawdown in hydraulic head in a confined aquifer at any radial distance from a well for any time after the beginning of pumping while assuming the medium as uniform and isotropic (i.e., equal in all directions). The Cooper-Jacob method (Cooper and Jacob, 1946), which is based on the Theis Method (Theis, 1935) but uses the late-time data, also assumes homogeneous media for confined aquifers. The Cooper-Jacob method however simplifies the analysis of pumping tests because the late-time drawdown is a linear function of time when plotted on a semi-log plot.

As noted above, these models are idealized solutions of the real system that are based on the assumption of homogeneity of the subsurface system. They are capable of producing accurate estimates of the flow if the aquifer is indeed homogeneous. Field data however shows that aquifer systems are almost always heterogeneous (Dagan, 1989; Gelhar 2003; Rubin 2003).

3.2. Stochastic Modeling Approach for Groundwater Problems

The heterogeneity and anisotropy of the aquifer systems and the lack of detailed data from field investigations inevitably result in high levels of uncertainty and non-uniqueness problems in the definition of the flow parameters (Gelhar, 1993; Rubin, 2005). In order to address the uncertainty and non-uniqueness of the parameters, researchers in the past two or three decades have developed stochastic approaches for the modeling of flow and transport. They pointed out that conventional deterministic methods that predict with no uncertainty the outputs for fixed model inputs may not be realistic, especially for large and complex applications (Rubin, 2005). On the other hand, stochastic approaches have been favored by an increasing number of researchers because the data are defined as probability distributions rather than single results (Younger, 2007). Uncertainty and randomness in the outcomes of the stochastic modeling approaches are a realistic reflection of the spatially variable structure of the hydraulic parameters and our incomplete definition of these parameters (Dagan, 1989; Hoeksema and Kitanidis, 1984).

3.2.1. Geostatistical Approach

One of the most commonly used stochastic modeling approaches is geostatistics. Geostatistics is a statistical discipline applied to earth systems that deals with the analysis and the prediction of spatial and temporal data. Geostatistical studies include exploratory data analysis, and evaluation of the spatial variability of attributes, and making simulations and predictions (Yeh et al.,1995; Kitanidis, 1997; Sanchez-Vila, 1999; Bohling, 2005).

Geostatistics is currently applied in many disciplines such as hydrology, hydrogeology, geochemistry, mining and agriculture. Geostatistical estimation methods contribute to the modeling efforts by offering how to use the data to compute the best estimates and, equally important, they provide a measure of the errors or uncertainty of these estimates (Kitanidis, 1997).

The Monte Carlo method is one of the most commonly used methods for assessing the uncertainty in the output of a model as a result of uncertainty in the definition of input parameters (Metropolis and Ulam, 1949; Mosegaard and Tarantola, 1995). In a Monte Carlo approach, multiple values of the input parameters are randomly generated based on their probabilistic distributions. The governing equations are then solved for each set of input parameters. The resulting output is then analyzed statistically to evaluate the resulting potential uncertainty in the model output. In order to observe the uncertainty of model parameters, Monte Carlo techniques can easily handle large input variances. Furthermore, to reflect all possible parameter values, a large number of realizations, in some instances more than one thousand realizations (the yield of each run is called “realization”) are necessary to see the probability distribution of outputs corresponding to each input (Elfeki et al., 1997).

3.2.2. Stochastically Interpretation of Pumping Test Data

There has been significant interest in the last decades in the analysis of pumping test head and drawdown data, particularly for the interpretation of pumping tests in heterogeneous porous media. Initial studies (Vandenberg, 1977; Barker and Herbert, 1982; Butler, 1988; Butler and Liu, 1993) considered different uniform aquifers separated with sharp inclusions. The effect of the transmissivity of the inclusions was valid for local scales and very short times. For long-time pumping tests, however, it was observed that the slope of drawdown versus log time was unaffected by the discontinuity of transmissivity values.

It has been proposed in recent years that pumping test interpretation techniques may be used to estimate the statistical spatial structure of the flow parameters. In geostatistical techniques, the spatial variability of attributes such as transmissivity, elevation, temperature or concentration is defined in terms of a statistical spatial structure. The statistical structure is commonly defined in terms of few statistical parameters such as the spatial mean, integral scale and variance of the attribute. The spatial mean defines the central tendency of an attribute while the variance is related to the amplitude of the variations of the attribute around its mean. The third parameter, the integral scale or sometimes referred to as the correlation length, describes the spatial pattern of these variations. It also gives the separation distance beyond which the attributes become statically uncorrelated (Renard, 2007).

Geostatistical tools have been used in the interpretation of pumping tests in heterogeneous aquifers. Some of the more relevant studies are mentioned below. Kitanidis (1986) and Feinerman et al. (1986) have applied Bayesian geostatistical approach in order to solve groundwater inverse problems. Schad and Teusch (1994) developed a method based on a definition of spatial and temporal scale. Their method provides a statistical description with a qualitative interpretation of the parameter distributions determined. They interpret drawdown and flow parameters over an increasing volume and changing depression cone with time. Meier et al. (1998) and Sanchez-Vila et al. (1999) analyzed numerical simulations of pumping tests and showed that the estimated transmissivity using conventional techniques such as Theis and Cooper-Jacob methods is close to the spatial geometric mean of the transmissivity field, T_{geo} . They showed that the storativity depends on the aquifer volume between pumping and observation wells however the transmissivity depends on the whole flow domain. The storativity estimates stabilize faster than the transmissivity estimates that approach a value that is close to the geometric mean. Moreover, the transmissivity estimated from the late drawdown data and the Cooper-Jacob method are practically independent of the location of the observation point, while the estimated storativity is space-dependent.

Given the complex relationship between hydraulic head and spatial flow parameters, particularly when the aquifer is heterogeneous, some researchers have used the concept of sensitivity coefficients. In complex modeling, sensitivity analysis can also

identify which parameters among many influence the dependent variables (Hornberger and Spear, 1981). For radially convergent flow towards a pumping well, Oliver (1993) evaluated numerically the sensitivity of variation of the transmissivity and storativity on the transient drawdown by using the Frechet kernel. Leven and Dietrich (2006) showed the effect of spatial variability of the transmissivity and storativity of a confined aquifer on the interpretation of single-well and two-well pumping tests by using sensitivity coefficients. Dagan (1989) and Gelhar (1993) analyzed the groundwater flow equations stochastically by interpreting the multivariate probability distribution of the dependent storativity and transmissivity variables. Rubin (2003) and Zhang (2002) used geostatistics to evaluate the impact of heterogeneity on contaminant transport.

It has been proposed in recent years that pumping test interpretation techniques may be used to directly estimate the statistical spatial structure of the flow parameters. Copty and Findikakis (2004a; 2004b) estimated the statistical spatial structure of the local scale log-transmissivity by using the transient drawdown data from pumping tests. They developed a Bayesian approach to estimate probability density functions for the statistical parameters, namely: the variance and integral scale. The method of Neuman et al. (2004; 2007) uses a graphical approach in order to estimate geometric mean, integral scale, and variance of the local log transmissivity by using quasi steady-state head data from pumping tests held in a confined, heterogeneous aquifer. Riva et al. (2009) applied the type-curve method developed earlier by Neuman et al. (2004) to field data and used it to estimate the mean drawdown and associated variance. Firmani et al. (2006) used an analytic expression of the equivalent hydraulic conductivity for steady-state radially convergent flow towards a well in a heterogeneous aquifer to estimate the variance and integral scale of the hydraulic conductivity.

3.3. Hydraulic Tomography

In parallel to all efforts to develop new pumping test interpretation techniques, some researchers have focused on the development of new field data acquisition technique for heterogeneous aquifer systems such as hydraulic tomography. Hydraulic tomography

involves pumping test at one of a series of wells and observing the drawdown due to pumping at adjacent wells (Gottlieb and Dietrich, 1995; Butler et al., 1999; Yeh and Liu, 2000; Bohling et al., 2002). While applying the hydraulic tomography method, water is sequentially pumped from or injected into an aquifer at different points of the aquifer (Figure 3.2). During each pumping test, hydraulic head responses of the aquifer at adjacent points are monitored and a set of head data are obtained. This procedure is repeated for all available wells; yielding many head data sets. The drawdown measurements from the entire set are then used in an inverse procedure to estimate the spatial variability of the parameters. Thus detailed knowledge about head responses due to pumping at a specific location can be provided and many data sets of head responses at different locations can be obtained by changing the position of the pumping test. Consequently, higher resolution of the distribution of parameters than conventional methods' distribution results is provided (Yeh and Liu, 2000).

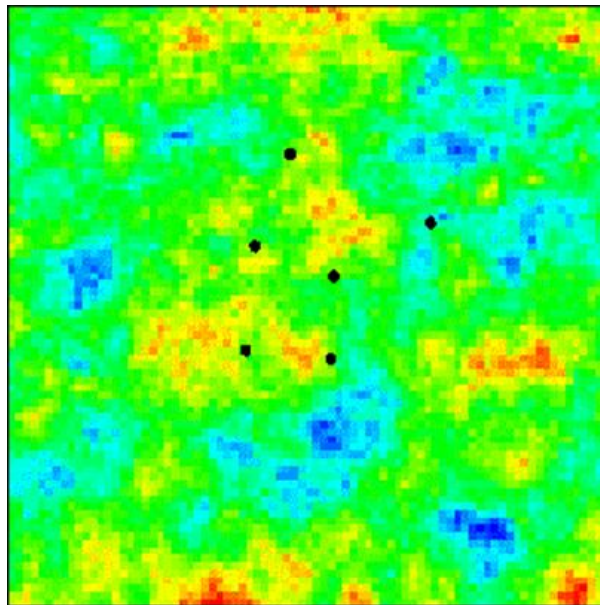


Figure 3.2. Multiple wells located on a synthetically-generated transmissivity field for use with hydraulic tomography.

Several researchers have proposed methods for the interpretation of hydraulic tomography. For example, Gottlieb and Dietrich (1995) investigated hydraulic tomography in order to identify the permeability distribution in a hypothetical, two dimensional saturated soil. They used a least squares-based inverse approach to create an image of the

spatial distribution of hydraulic conductivity. Butler et al. (1999) used hydraulic tomography to networks of multilevel sampling wells. They proposed new techniques for measuring head data at a scale that had previously been unobtainable. Their new methodology greatly facilitated the implementation of hydraulic tomography in the field. Yeh and Liu (2000) interpreted the results of hydraulic tomography by developing an iterative geostatistical inverse method. They proved their hydraulic tomography interpretation technique can reveal more detailed aquifer heterogeneity than conventional aquifer tests. In the study of Bohling et al. (2002), the value of the steady state concept for inversion of hydraulic tomography data was demonstrated and its robustness with respect to improperly specified boundary conditions was investigated.

4. METHODOLOGY

This chapter describes the methodology used for the interpretation of pumping test data from heterogeneous confined aquifers. Section 4.1 describes conventional methods for the interpretation of time-drawdown data that are commonly used in actual field applications. These methods are based on the assumption of homogeneity of the aquifer volume and hence yield single average estimates of the flow parameters. Section 4.2 describes a novel method that focuses on the estimation of the variability of the transmissivity as a function of distance from the pumping well. In order to estimate the parameters of the statistical spatial structure, namely: integral scale and variance, two approaches were considered: a weighted least-squares approach and a Bayesian approach. These two approaches are described in Section 4.3. All the developed methods used synthetically generated pumping tests data for evaluation. The methods used to generate the heterogeneous transmissivity fields and the pumping test data are described in Section 4.4.

4.1. Conventional Methods for Confined Aquifers

A confined aquifer is an aquifer that is bounded above and below by impervious formations. In a confined aquifer, the water level in a well rises above the top of the aquifer, in some cases even above the ground surface, because the pressure of the water is generally higher than the pressure of the atmosphere (Batu, 1998). When a well taps the aquifer, due to the compressibility of the aquifer material and the water, hydraulic head changes rapidly.

The drawdown due to pumping is measurable at considerable distances from the well (Figure 4.1). In order to interpret the pumping tests, the Theis (1935) method and Cooper-Jacob (1946) method are two of the most preferred conventional techniques provided the aquifer is non-leaky and unbounded and the flow is non-steady. These two

techniques which are widely used in field applications because of their relative simplicity are briefly described below.

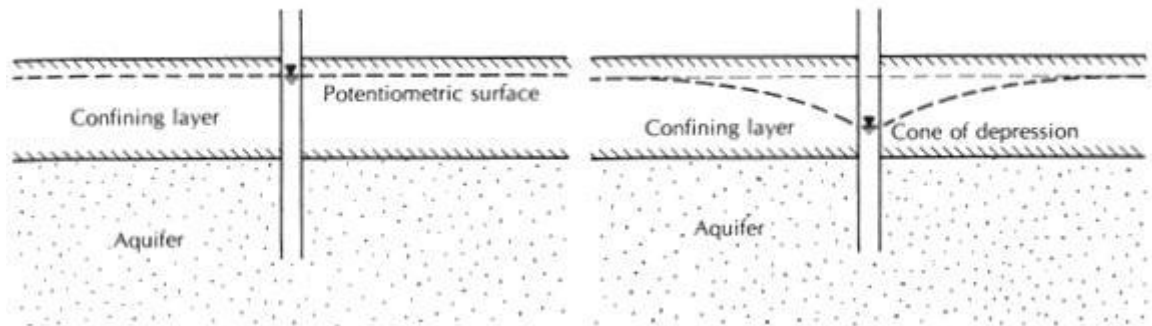


Figure 4.1. Drawdown change in a confined aquifer (Fetter, 2001).

4.1.1. Theis Method

The first analytical solution of transient drawdown in a confined aquifer was developed by Theis (1935). He made an analogy between heat flow and groundwater flow by assuming temperature is analogous to head. Theis formulated a method for determining the transmissivity and the storativity for fully penetrated confined aquifers under the following assumptions:

- The aquifer is homogeneous, horizontal, not leaky, unbounded and isotropic.
- The aquifer has a constant thickness.
- The aquifer is pumped at a constant discharge rate.
- Piezometric surface is the same at every point in the aquifer before the pumping test.
- Decreasing head is proportional to the storage in the aquifer.

For the given conditions, the drawdown as a function of time can be written as;

$$s(r,t) = h_0 - h(r,t) = \frac{Q}{4\pi T} \int_{\infty}^u \frac{e^{-y}}{y} dy \quad (4.1)$$

$$s(r,t) = \frac{Q}{4\pi T} W(u) \quad (4.2)$$

where

s	transient drawdown
h	hydraulic head
h_0	initial hydraulic head
Q	constant discharge rate
T	transmissivity
S	storativity
t	time
r	radial distance from the pumping well
u	dimensionless time factor, $\frac{r^2 S}{4Tt}$ (For constant S and T , $1/u$ is equivalent to non-dimensional time).
$W(u)$	well function

To interpret a pumping test with the Theis method, a $W(u)$ versus $1/u$ (non-dimensional time) plot on a log-log scale is used. A sample plot of $W(u)$ versus $1/u$ is shown in Figure 4.2. The theoretical well function on the graph is matched with the observed drawdown data as a function of time also plotted on a log-log scale graph. After selecting a matching point on both graphs, the storativity and transmissivity estimates are calculated from the coordinates of the matching point.

In applying Theis' method, the theoretical equation is based on the condition that the well discharge remains constant during the test. However, real flow conditions may vary and create a time lag in order to adjust the pressure decline. Thus a disagreement

between measured results and theoretical plot may occur at earlier times. After the time of the test becomes larger these affects are minimized and the real and theoretical results get closer.

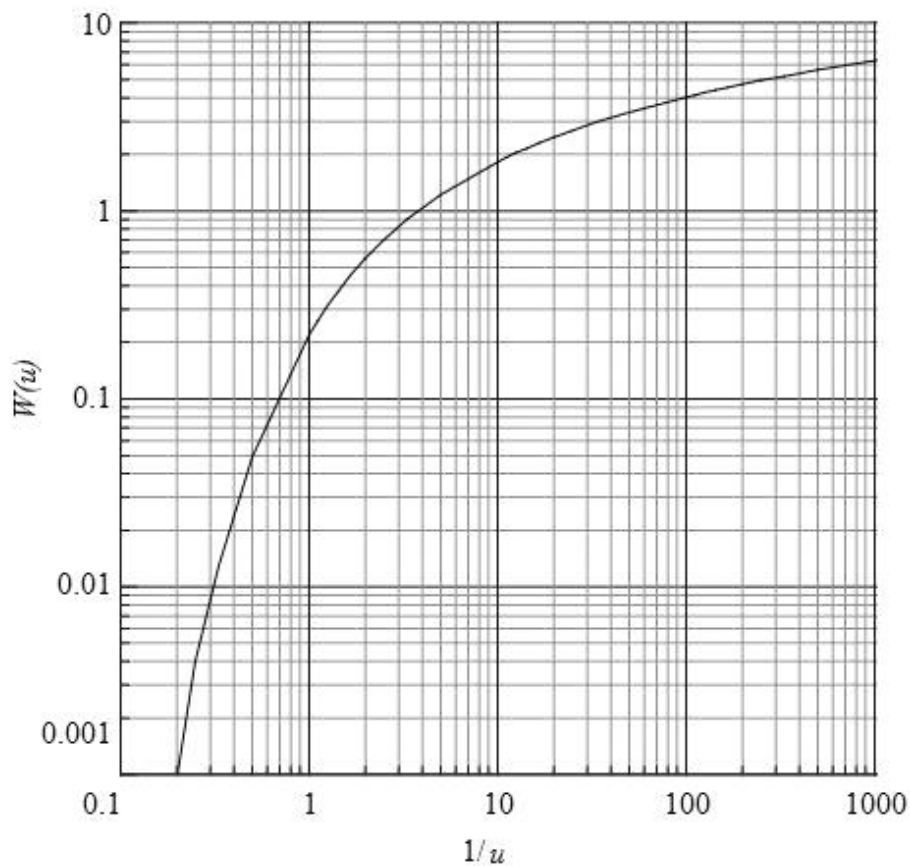


Figure 4.2. Theis curve (Batu, 1998).

4.1.2. Cooper-Jacob Method

An approximation for the Theis equation and a developed interpretation method that does not require type-curve matching were derived by Cooper and Jacob (1946). By assuming the same conditions as the Theis method and small values for radius (r) and large values for time (t), they developed this technique. Thus they neglected earlier times of the constant-rate pumping tests and they provided an approximation by taking straight line

segment of Theis function at late times when plotted on a semi-log plot. The approximated equation for the straight-line segment is:

$$s = \frac{2.3Q}{4\pi T} \log \frac{2.25Tt}{r^2 S} \quad (4.3)$$

This method consists of plotting the data of the drawdown versus time, the latter on a logarithmic scale (Figure 4.3). Using the interception and the slope values of fitted straight line, the transmissivity and the storativity values are estimated from the equation (4.3). After the estimation of the T and S values, the condition for the applicability of the method is checked in dimensionless time factor “ u ”. The value of “ u ” should be less than 0.01 (equivalent to late time).

The results of this interpretation method that considers a single pumping test drawdown data demonstrate that the values are obtained under the homogeneity assumption. However, in pumping tests conducted in heterogeneous media transmissivity and storativity values show variability, especially storativity estimates may display very large variability (Meier et al., 1998).

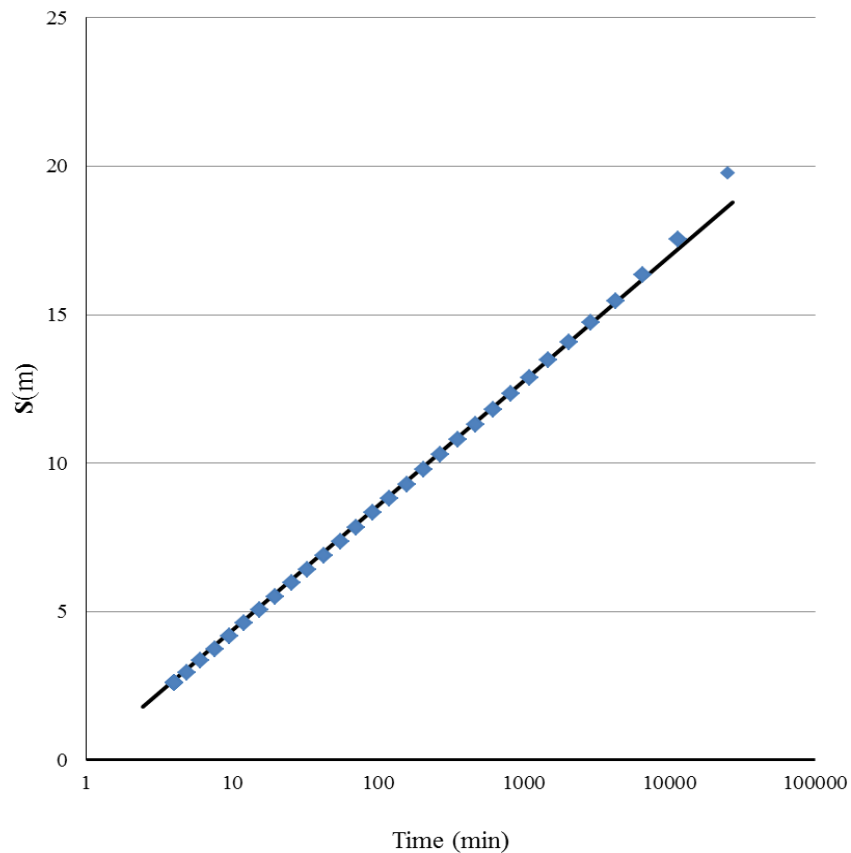


Figure 4.3. An example for Cooper-Jacob straight-line fitting (Batu, 1998).

4.2. Novel Methods for Confined Aquifers

Field investigations have shown that natural geologic systems are almost always heterogeneous with flow parameters that vary in complex spatial patterns. Moreover, groundwater flow and contaminant transport are strongly influenced by the heterogeneity of the flow parameters. Therefore, there is a need to develop novel techniques that focus on providing some information about the variability of the flow parameters, especially the transmissivity. This section describes a novel technique that uses the drawdown and its time derivative to estimate the flow parameters in the vicinity of the pumping test as a function of distance from the pumping well.

4.2.1. Continuous Derivation Method

The Continuous Derivation (CD) method is a novel procedure for the interpretation of pumping tests in heterogeneous and confined aquifers (Coptý et al., 2011). Because conventional methods attempt to estimate a single estimate for the flow parameters even though the aquifer is not homogeneous, this method is developed to signify the presence of heterogeneity for groundwater flow and contaminant transport. Conventional pumping tests analysis methods use drawdown data collected at different times as a way for the estimation of representative values of the flow parameters. For instance, type-curve fitting graphical methods fit the drawdown data to normalized drawdown curves. The Cooper-Jacob method attempts to fit a straight line to the late-time drawdown data. Such methods assume that the subsurface systems are formed by one or at most a few homogeneous units.

However, the estimates vary as the drawdown cone of depression expands in time. At earlier times estimated transmissivity is close to the transmissivity at the well while at later times it is some weighted spatial mean of the transmissivity in a much larger region around the well. The effect of the weighted spatial mean is related with the locations of the pump and observation wells, the integral scale and the transmissivity variance.

The Continuous Derivation method claims that a heterogeneous aquifer can be represented by a homogeneous one whose flow parameters evolve in time as the cone of depression expands in time. It is based on the use of the ratio of the drawdown to the drawdown derivative. In this method, each storativity and transmissivity parameter are estimated at a specific time. By repeatedly taking the ratio of the drawdown to the drawdown derivative, the time-dependent storativity and transmissivity parameters will be estimated as a function of radial distance from the well (Coptý et al., 2011). Then the estimates are compared with the spatial average of the transmissivity around the well. By using synthetic pumping tests with known transmissivity distributions, one is able to assess the validity and robustness of the estimation method.

In order to obtain the ratio of the drawdown to the drawdown derivative, the CD method starts with the equation (4.1) for the transient drawdown in a confined aquifer. The first derivative of the drawdown as a function of log of time is calculated as:

$$s' = \frac{ds}{d \log T} = \frac{2.3Q}{4\pi T} \exp(-u) \quad (4.4)$$

The ratio of the drawdown and its derivative (γ_c) at the considered time is found by dividing the equation (4.1) to the equation (4.4):

$$\gamma_c = \frac{2.3s}{s'} = W(u) \exp(u) \quad (4.5)$$

Figure 4.4 shows the plot of γ_c as a function of $1/u$. γ_c increases monotonically as dimensionless $1/u$ increases. At any particular time the procedure starts first by estimating the drawdown derivative at that particular time from the observed drawdown. Next, γ_c at that particular time is estimated from the ratio of the observed drawdown and its derivative. From the computed value of γ_c one can determine the value of u^* using the graph of γ_c shown in Figure 4.4, and the corresponding well function $W(u^*)$. Then the transmissivity and the storativity are estimated as:

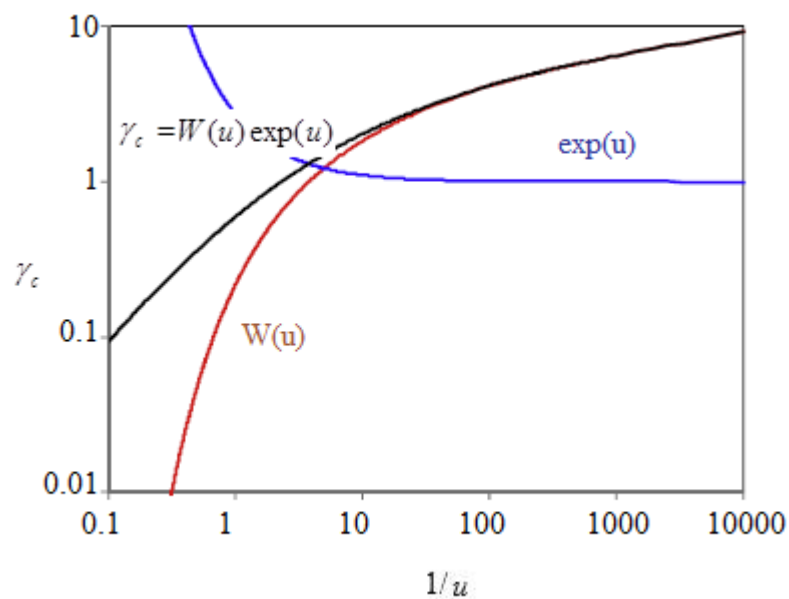


Figure 4.4. The plot of γ_c as a function of $1/u$.

$$T_i = \frac{Q}{4\pi s(t)} W(u^*) \quad (4.6)$$

$$S_i = \frac{4tT_i u^*}{r^2} \quad (4.7)$$

Hence, the steps of the CD method to estimate the transmissivity and storativity values are summarized below:

- u^* is calculated from the plot of the ratio of s/s' at any time.
- transmissivity is calculated from equation (4.6) and the the corresponding value of $W(u^*)$
- storativity is calculated using equation (4.7).

The above procedure is applied for all available times since the start of pumping until the pumping test is terminated. Hence, the procedure allows for the continuous estimation of the flow parameters as a function of time in contrast to conventional methods which only provide a single average estimate of the parameters.

In order to convert the estimates of the flow parameters as a function of time into functions of distance, the following equation is used (Copty et al., 2011):

$$r^* = \sqrt{\frac{4tT}{1.65S}} \quad (4.8)$$

where r^* is the distance calculated, T and S are the time-dependent transmissivity and storativity and t is the considered time.

4.3. Estimation of Integral Scale and Variance

Two approaches were used to estimate the two statistical parameters defining the transmissivity semi-variogram -namely the integral scale and the variance- from the estimated transmissivity (T_e) as a function of radial distance. The first approach is a least-squares estimator while the other relies on Bayes' theorem on conditional probability. The estimates of the integral scale and the variance were obtained by comparing the transmissivity estimates as a function of distance, $T_e(r)$ to the spatial average of the transmissivity, referred to as the theoretical transmissivity as a function of radial distance, $T_{th}(r)$. $T_{th}(r)$ was computed by simulating multiple realizations of the transmissivity (1000 realizations), taking the spatial average of the transmissivity of each realization as a function of radial distance and then averaging over the 1000 realizations. This was performed for different integral scale and variance values. Figure 4.5 shows the family of theoretical curves T_{th} , for the variance values ranging from 1 to 4. The impact of the integral scale is then seen in the x-axis which is expressed as non-dimensional time, r/I .

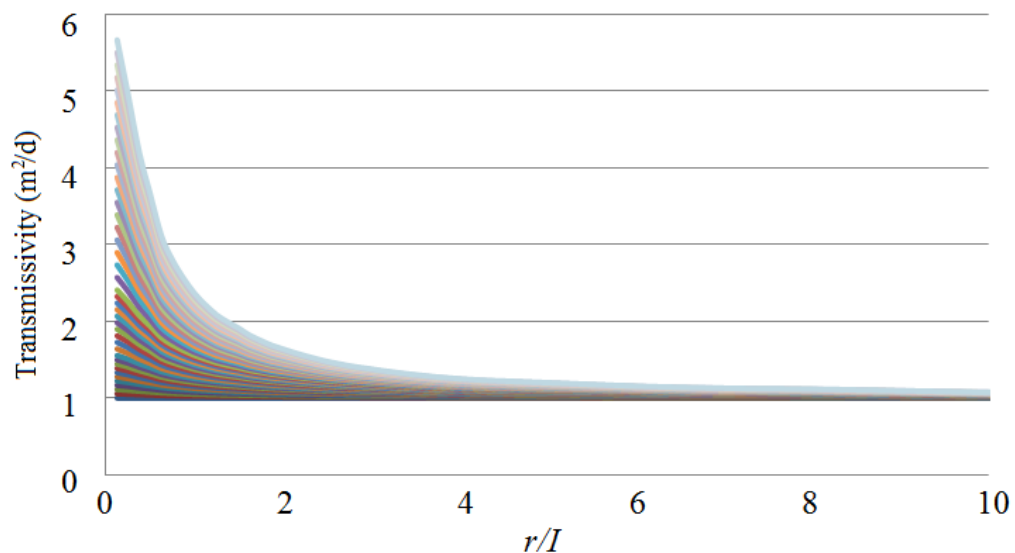


Figure 4.5. Theoretical transmissivity curves consisting of the geometric mean of the transmissivity as a function of radial distance for different values of variance and integral scale.

The following sections describe the two approaches for the estimation of the variance and integral scale.

4.3.1. Weighted Least-Squares Approach

The first approach used for the estimation of the integral scale and the variance is a weighted least-squares approach. In order to apply this approach, $T_e(r)$ was obtained from each pumping test as described in Section 4.2.1 firstly. On the other hand, a family of curves of $T_{th}(r)$ was obtained for different variance and integral scale values (Figure 4.5). These curves were estimated from the generated transmissivity fields whereas $T_e(r)$ was obtained from the interpretation of the simulated pumping tests. As will be demonstrated later, $T_e(r)$ is a good estimate of $T_{th}(r)$ which serves as a basis for comparing $T_e(r)$ to the theoretical curves shown in *Figure 4.5*.

To estimate the integral scale and the variance, $T_e(r)$ were matched with the $T_{th}(r)$. Then, a weighted least-squares difference between $T_e(r)$ and $T_{th}(r)$ was computed:

$$\sum_1^n \frac{|T_{th} - T_e|^2}{\sigma^2} \quad (4.9)$$

Weighting was taken to be inversely proportional to the variance (from 1 to 4) associated with each curve to account for the spread in individual simulations used in the estimation of $T_{th}(r)$. The squared differences were calculated for each indicated distance and then summed up. The best estimates of the integral scale and the variance were selected such that the sum of the squared differences is minimized. Single as well as multiple pumping tests were considered. When multiple tests were available, $T_e(r)$ from individual tests was first estimated and their average was compared to $T_{th}(r)$ using equation (4.9). It was assumed that 1, 5 and 10 multiple tests were available. The latter two cases correspond to hydraulic tomography consisting of 5 and 10 tests, respectively.

4.3.2. Bayesian Approach

The second approach uses a bayesian formulation for the estimation of the integral scale and variance. The Bayesian approach computes first the probability density function (pdf) of $T_{th}(r)$ from the 1000 transmissivity realizations. From this pdf and $T_e(r)$, the probability of occurrence of the integral scale and variance are computed. This is in contrast to the least-squares approach which uses the 1000 transmissivity realizations to calculate an average (Figure 4.5) and then comparing $T_e(r)$ to this average.

To better clarify the Bayesian approach, we start with the definition of Bayes' theorem which can be written as:

$$P(A/B) = \frac{P(A \cap B)}{P(B)} \quad (4.10)$$

In words, this means that the probability of event A given event B is equal to the joint probability of events A and B divided by the probability of event B. Similarly,

$$P(B/A) = \frac{P(A \cap B)}{P(A)} \quad (4.11)$$

From Equation 4.10 and 4.11, we can write:

$$P(A/B) \times P(B) = P(B/A) \times P(A) \quad (4.12)$$

Rearranging the terms in equation 12 yields:

$$P(A/B) = \frac{P(B/A) \times P(A)}{P(B)} \quad (4.13)$$

Therefore equation (4.13) allows us to estimate the probability of event A given event B in terms of the probability of event B given event A. In many applications, such as parameter

estimation problems, this result can be quite useful because it allows writing the inverse problem (the parameter estimation problem) in terms of the forward problem. In our case, we can use Bayes' theorem to write:

$$P(\sigma^2, I / \psi) = \frac{P(\psi / \sigma^2, I) \times P(\sigma^2, I)}{P(\psi)} \quad (4.14)$$

where Ψ stands for the estimated transmissivity $T_e(r)$ derived from a pumping test.

In words, equation (4.14) says that the probability of the variance and integral scale (σ^2, I) equal to some values given $T_e(r)$ can be expressed in terms of the probability of $T_e(r)$ given the variance and integral scale values. In the equation, $P(\sigma^2, I)$ denotes the prior joint probability of the variance and integral scale which represents our knowledge of these two parameters prior to the pumping test. In this calculation, this prior distribution was assumed to be uniform (all values between the minimum and maximum have equal probability to reflect minimum information about their distributions). $P(\Psi)$ appearing in the denominator of the equation acts as a normalizing parameter that forces each probability term to be between 0 and 1 and also the sum of all probabilities equal to 1. $P(\Psi / \sigma^2, I)$ which is the probability of having a transmissivity estimate curve as a function of distance given some values of the integral scale and the variance, is estimated by generating many realizations of the transmissivity field for these particular values of integral scale and variance and calculating the pdf.

Finally, the expected values of the integral scale and variance were computed from the estimate probability density function of these two variables by using equations (4.15) and (4.16).

$$E[I] = \sum_I I \times P(I) \quad (4.15)$$

$$E[\sigma^2] = \sum_{\sigma^2} \sigma^2 \times P(\sigma^2) \quad (4.16)$$

4.4. Numerical Simulation

The focus of this thesis is on the development of a new method for the interpretation of drawdown data obtained from hydraulic tomography and the numerical testing and evaluation of this method. The development and numerical testing of this method for the estimation of the statistical spatial structure that describes the transmissivity field for confined and heterogeneous aquifers were performed by using synthetically-generated pumping test data. Pumping tests are generally expensive requiring extensive drilling and hence are not very readily available. The advantages of using synthetic data are:

- Numerous pumping tests can be easily simulated for different input parameters and conditions.
- By using synthetic data with known input parameters, the pumping tests interpretation methods can be more extensively evaluated, as we would be able to compare the estimated parameters with the actual parameters used in the data generation.
- Although the generated data are not “real”, extensive previous evaluation of the tools used have shown that these tools are quite robust and can produce data that are indeed close to “real” data obtained from the field. (Dagan and Neuman, 1997).

The main steps for the numerical simulation are:

- Heterogeneous transmissivity fields were generated using the turning bands method (Mantoglou and Wilson, 1982). It was assumed that the natural log transform of the transmissivity (Y) is a multivariate Gaussian random spatial function with zero mean ($T_{geo}=1$), with an exponential semi-variogram, with variance of $\sigma^2= 1, 2$ and integral scale $l=8$ and 24 length units. The exponential semi-variogram $\gamma(h)$ as a function of distance can be written as;

$$\gamma(h) = \sigma^2 \left(1 - \exp\left(-\frac{h}{l}\right) \right) \quad (4.17)$$

where the variance $\sigma^2 > 0$ and the integral scale $I > 0$ (Kitanidis, 1997).

- Using the pixelplot program of GSLIB, a geostatistical software library program, selected heterogeneous transmissivity fields were plotted (Deutch and Journel, 1992).
- By using the generated transmissivity distributions as input, pumping tests were simulated with the MODFLOW (McDonald and Harbaugh, 1988; Harbaugh et al., 2000) a computer code written in FORTRAN language and that can simulate the groundwater flow through porous media. It solves the groundwater flow partial differential equation with different possible properties, boundary and initial conditions. The program solves the following equation:

$$\frac{\partial}{\partial x} \left(K_x \frac{\partial h}{\partial x} \right) + \frac{\partial}{\partial y} \left(K_y \frac{\partial h}{\partial y} \right) + \frac{\partial}{\partial z} \left(K_z \frac{\partial h}{\partial z} \right) = S_s \frac{\partial h}{\partial t} \quad (4.18)$$

where

h	hydraulic head
K	hydraulic conductivity along the x , y and z directions
S_s	specific storage coefficient

- A Monte Carlo approach was used in order to generate multiple realizations of the transmissivity and simulate the pumping tests. By repeating the analysis for a large number of cases, we are able to better assess the robustness of the proposed method.
- For the interpretation of the simulated pumping tests the Continuous Derivation (CD) method based on the use of the ratio of the drawdown to the drawdown derivative was used (Coptly et al., 2011).
- To estimate the integral scale and variance of the transmissivity field, two approaches were used: a weighted least-squares approach and a Bayesian approach. These two approaches are described in more detail in the above section. The estimated integral scale and variance were then compared to the “actual” parameters used in the transmissivity field generation.

The aquifer system was assumed as heterogeneous and confined. The transmissivity distribution was generated using the turning Bands Method as described above (Mantoglou and Wilson, 1982). The storativity on the other hand was assumed to be uniform as field data indicate that the spatial variation in the storativity varies much less than the transmissivity (Sanchez-Vila et al. 1999). The specific storage value used in all simulations was 0.0001, which is typical for confined aquifers (Domenico and Schwartz, 1997).

To simulate the pumping tests and the hydraulic tomography, full penetrating wells were located within the aquifer domain. The pumping rates were selected as either 1 or 2 m³/d.

Constant head conditions were defined along the outer boundaries of the flow domain. However, pumping tests were terminated before the prescribed boundary head conditions started to influence the solution. Two flow domains were considered: 481 x 481 m and 999 x 999 m. The flow domain was discretized using a uniform grid of 1 x 1 m. The larger domain allows for longer pumping tests. However, the larger domain requires longer simulation time.

For the simulation of the hydraulic tomography, it was assumed that 6 wells were present. The location of the wells was randomly generated such that they are not too close to the boundary or to each other. Pumping was from one well at a time sequentially. For each pumping well, the drawdown was simulated at all available wells.

By using the finite difference model MODFLOW program (McDonald and Harbaugh, 1988; Harbaugh et al., 2000) the governing partial differential equations defining groundwater flow in porous media were solved. For these simulations the duration of the tests was defined as two days and the initial water level was prescribed as 20 m. Drawdown data were simulated at the cells where the wells located in accordance with the hydraulic tomography method.

A summary of the main steps used in this study for the numerical simulations can be seen in Figure 4.6.

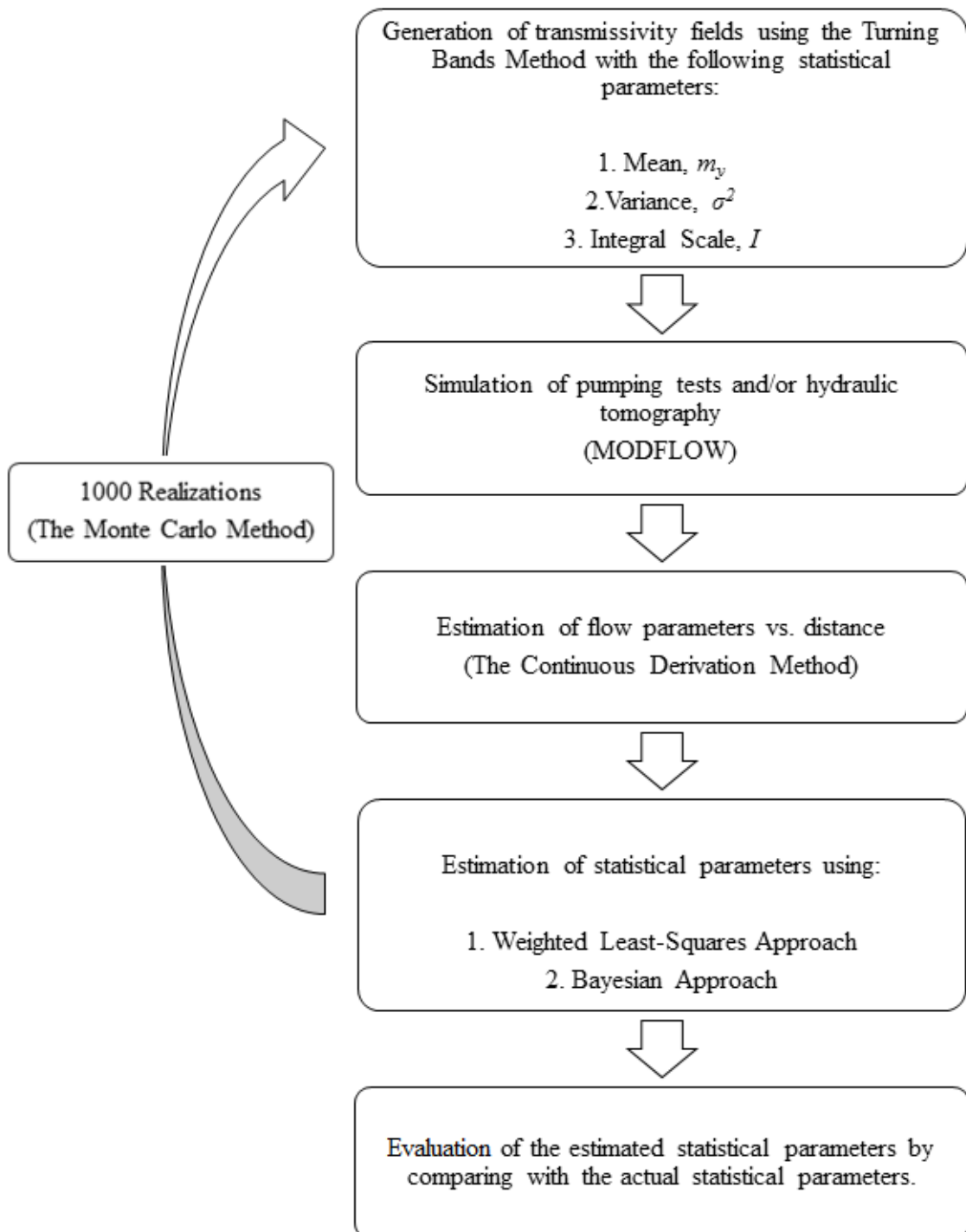


Figure 4.6. The flow chart showing the main steps of this study.

5. RESULTS AND DISCUSSION

This section presents the application of a novel pumping test interpretation method, namely the Continuous Derivation Method which uses the drawdown and its time-derivative to estimate the flow parameters (Copty et al., 2011). The method will first be applied to synthetically-generated single pumping tests as well as multiple pumping tests (hydraulic tomography). The method will then be extended to estimate the statistical spatial structure of the transmissivity from hydraulic tomography data. In order to estimate the statistical parameters of the heterogeneous transmissivity field (integral scale and variance) two different approaches are evaluated: (i) a weighted least-squares approach and (ii) a Bayesian approach. The advantage of using synthetically-generated pumping test data is that we can evaluate the performance of these two approaches by comparing the results to the original statistical parameters used in the data generation. This comparison is performed for many pumping tests with different input parameters to better evaluate the proposed pumping test interpretation method.

5.1. Generation of Transmissivity Fields

Heterogeneous transmissivity fields were randomly generated using the turning bands method as described in Section 4 (Mantoglou and Wilson, 1982). Using different variance and integral scale values, three sets of natural log transmissivity fields were generated:

- Set 1: mean, $m_y=0$; variance, $\sigma^2=1$; integral scale, $I=8$;
- Set 2: mean, $m_y=0$; variance, $\sigma^2=2$; integral scale, $I=8$;
- Set 3: mean, $m_y=0$; variance, $\sigma^2=1$; integral scale, $I=24$.

The above parameters are for the natural log-transform of the transmissivity, $Y=\ln T$. Note that the mean of the transmissivity was assumed to be $1 \text{ m}^2/\text{d}$ which corresponds to a

mean of the $\ln T$, $m_y=0$. The range of variances considered here is comparable to many of the values observed in the field (Gelhar 1993; Rubin 2003).

Figure 5.1 shows four realizations of the generated $\ln T$ fields. Although the same statistical parameters were used for the random generation of these fields, (namely, $m_y=0$, $\sigma^2=1$ and $I=8$), the four fields vary considerably, demonstrating the randomness of the generation procedure. Blue regions are regions of low transmissivity while red regions are regions of high permeability. The size of individual features in these domains is dependent on the value of I while the magnitude of the variations around the mean are function of the variance. The generated transmissivity fields are then used as input for the simulation of pumping tests.

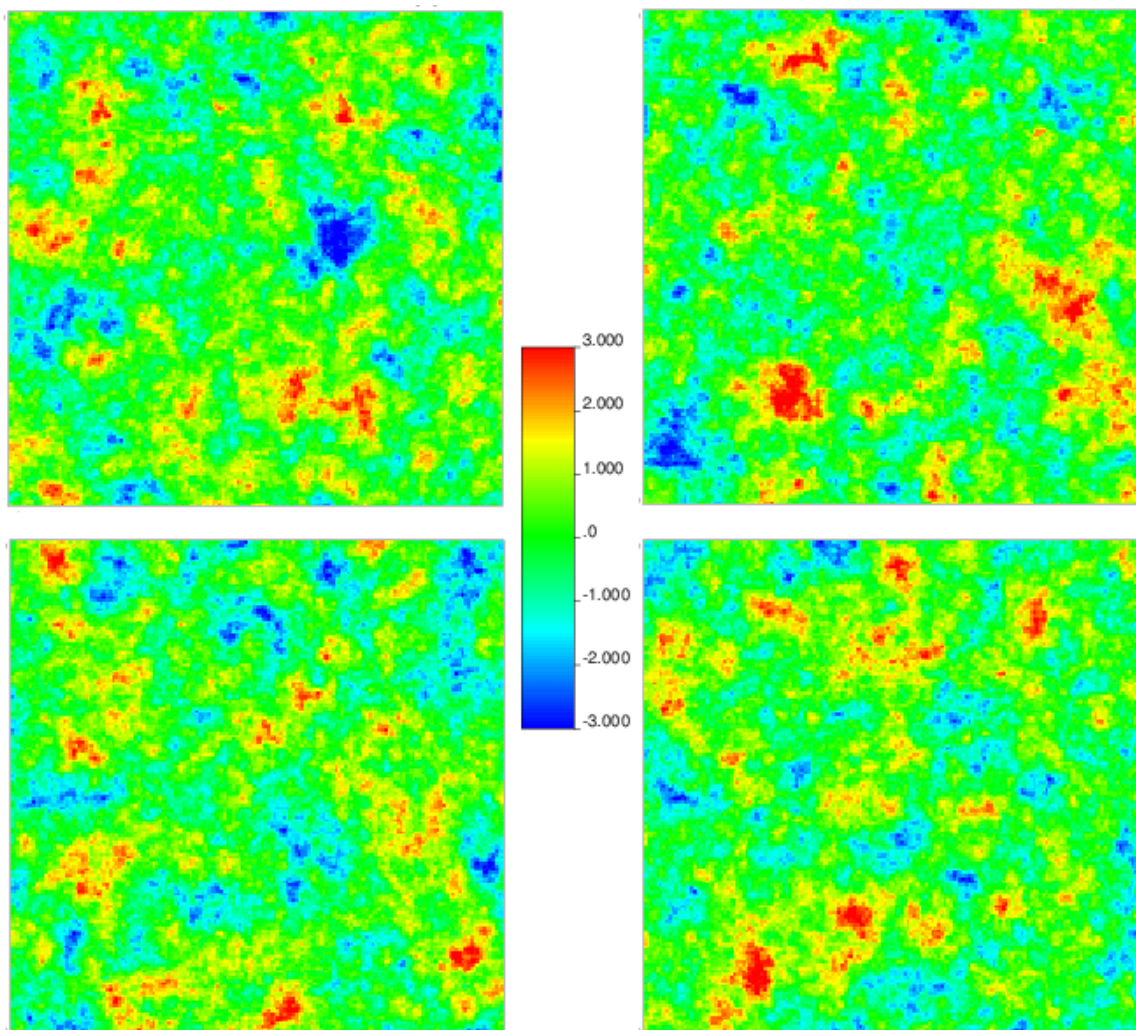


Figure 5.1. Randomly generated $\ln T$ fields with same mean, variance and integral scale values ($m_y=0$; $\sigma^2=1$; $I=8$).

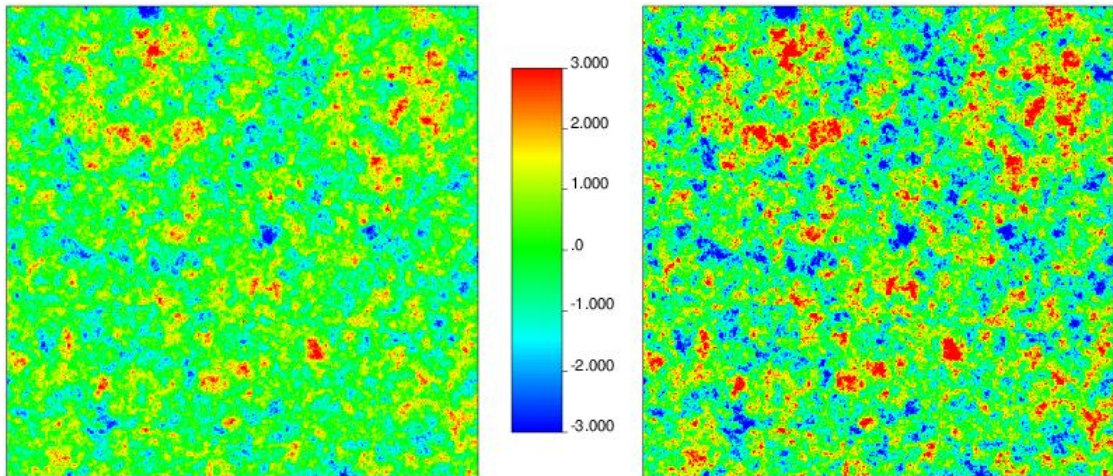


Figure 5.2. Effect of variance on the generated transmissivity fields with $\sigma^2=1, 2$ respectively.

Secondly, the effect of variance on the generated $\ln T$ fields is shown in Figure 5.2 which shows two fields with the same mean ($m_y=0$) and integral scale ($I=1$) but with two different variances: $\sigma^2=1, 2$ respectively. Figure 5.2 clearly displays that the field with higher variance value has larger variability in the transmissivity than the one with the lower variance.

To observe the influence of the integral scale, two $\ln T$ fields were generated with different integral scale values ($I=8$ and 24 respectively) but with the same mean ($m_y=0$) and variance ($\sigma^2=1$). From Figure 5.3, it can be seen that the integral scale describes the spatial pattern of the variations. Lower integral scale value results in larger variations of the transmissivity as a function of distance. For larger integral scales, variations are more gradual.

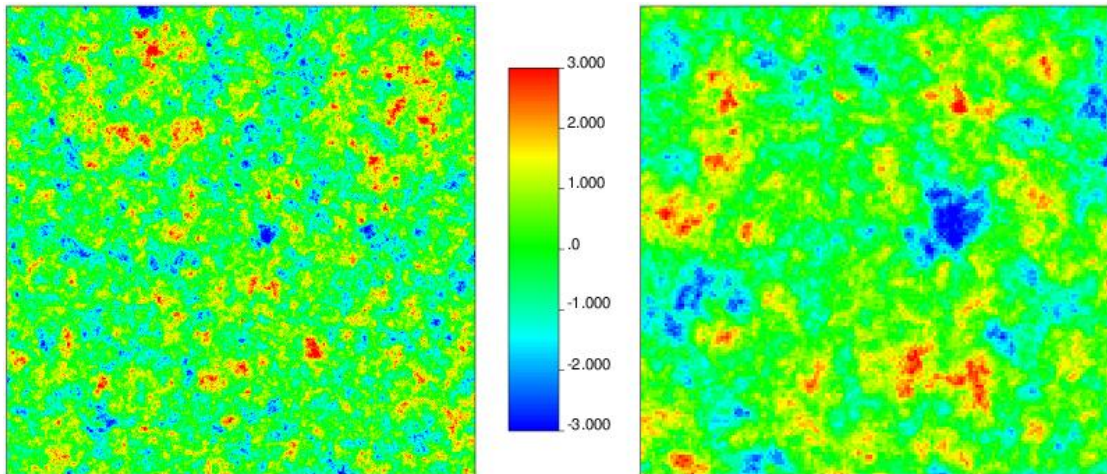


Figure 5.3. Effect of integral scale on the generated transmissivity fields with $I=1, 2$ respectively.

5.2. Hydraulic Tomography Results

For the simulation of the hydraulic tomography, it was assumed that 6 wells were available. Figure 5.4 shows the selected well locations superimposed over one of the randomly-generated transmissivity fields. In order to reduce the effect of the imposed boundary conditions, hydraulic tomography method has been applied to a transmissivity field with a very large domain (999 x 999 m). The wells selected to be about 32 m to 105 m which is typical for real field applications. Pumping was from one well at a time sequentially and for each pumping well, the drawdown was simulated at all available wells. The duration of each pumping test was 2 days.

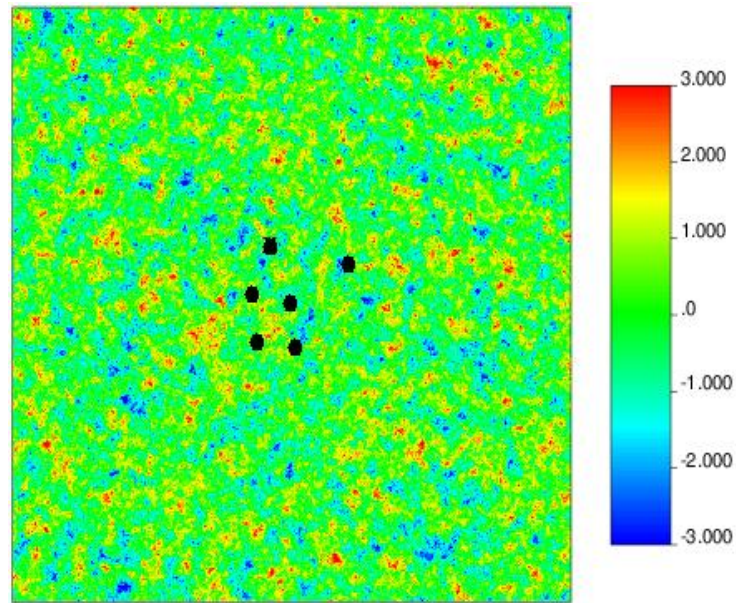


Figure 5.4. Location of wells (randomly selected) for hydraulic tomography superimposed over one of the randomly-generated $\ln T$ fields.

Figure 5.5 shows the simulated drawdown as a function time for each of the 6 pumping tests (referred to s1, s2 ... s6) and 6 observation wells. Generally, the largest drawdown is at the pumping well itself. The drawdown generally decreased as the distance between the observation well and the pumping well increased, but this is not always the case due to the heterogeneity of the flow field. Moreover, the drawdown looks generally smooth with time despite the fact that the transmissivity was spatially non-uniform. This is one of the main reasons why some researchers have proposed to use the drawdown derivative in the interpretation of pumping tests in heterogeneous aquifers.

For each of the pumping tests and observation wells, the transmissivity was estimated as a function of radial distance using the Continuous Derivation method. The estimated transmissivities are shown in Figure 5.6.

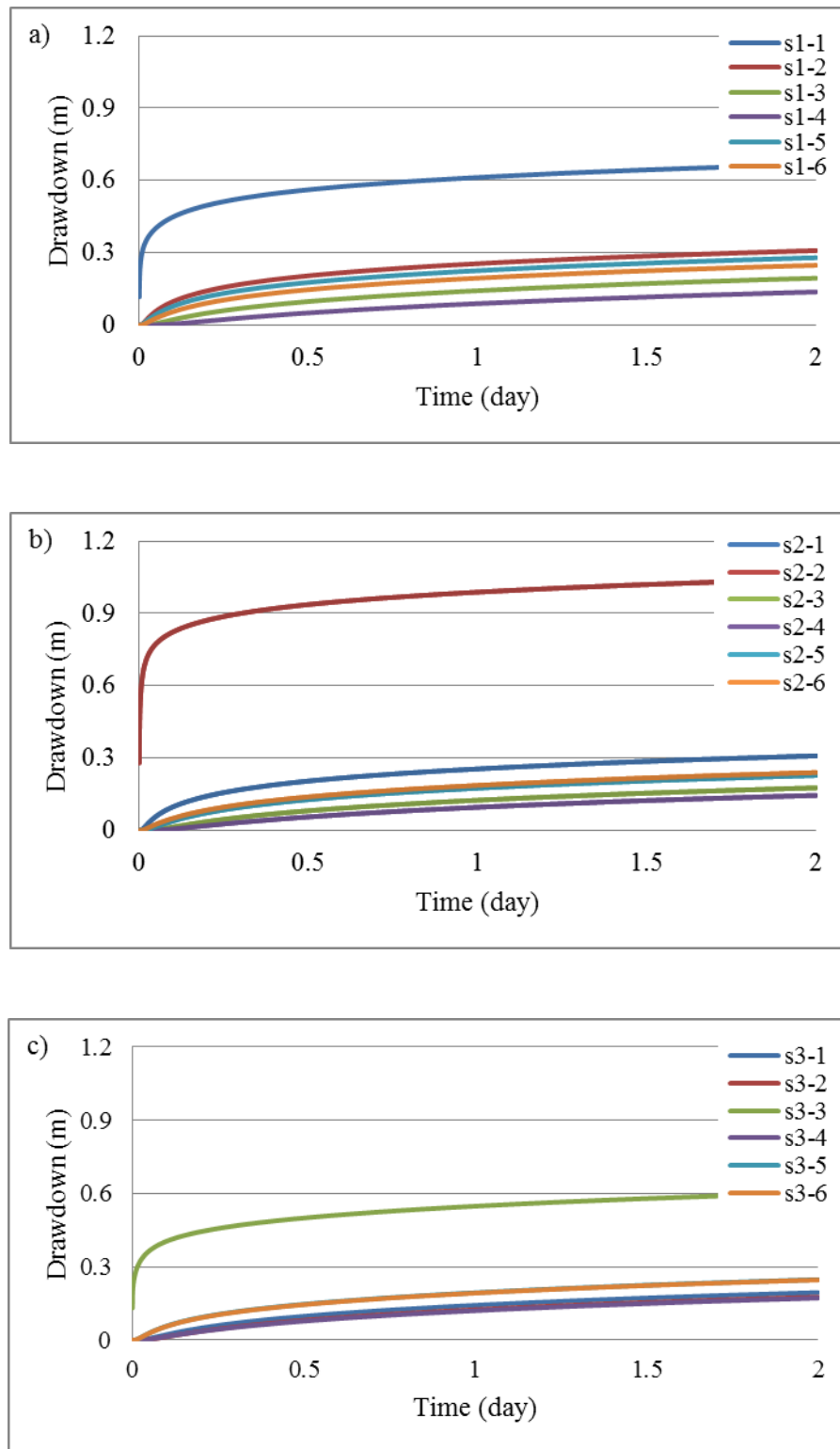


Figure 5.5. Drawdown results obtained from hydraulic tomography for a) Well-1, b) Well-2, c) Well-3.

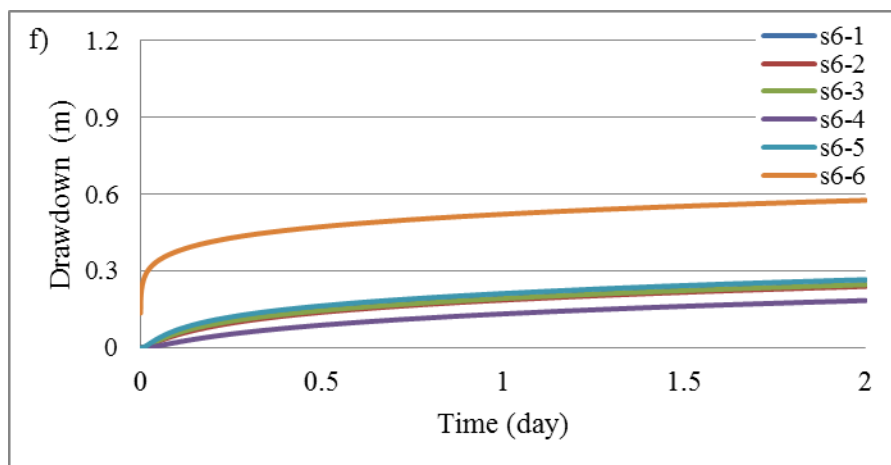
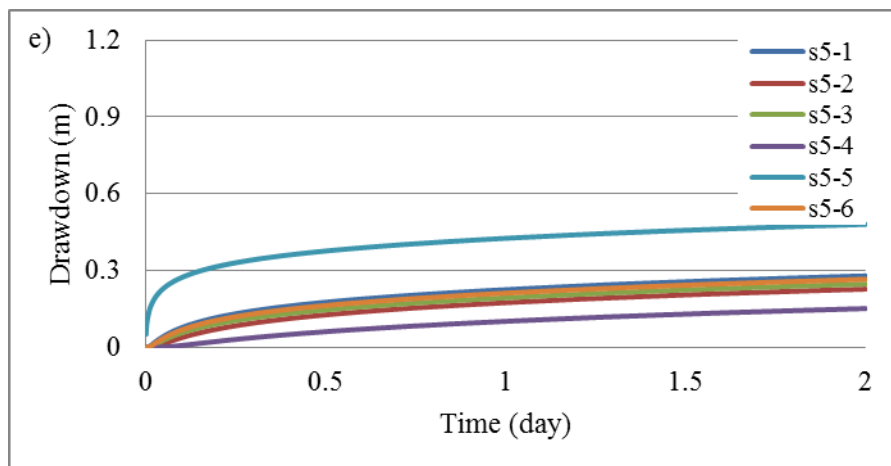
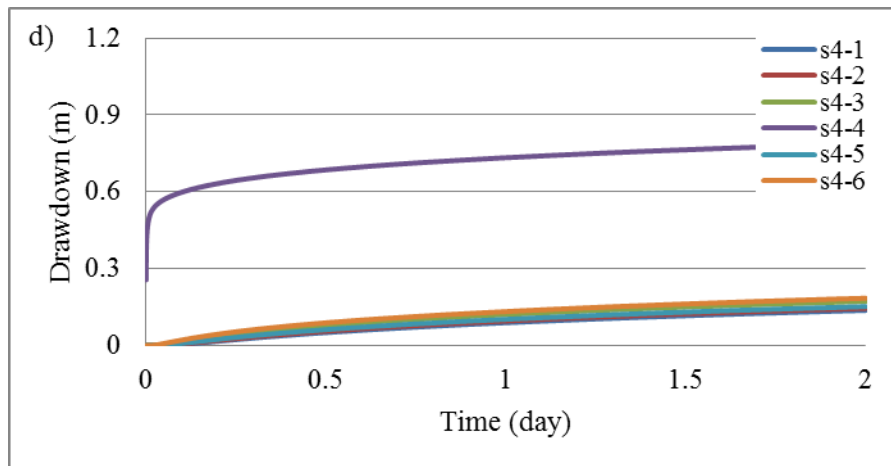


Figure 5.5. Drawdown results obtained from hydraulic tomography for d) Well-4, e) Well-5 and f) Well-6.

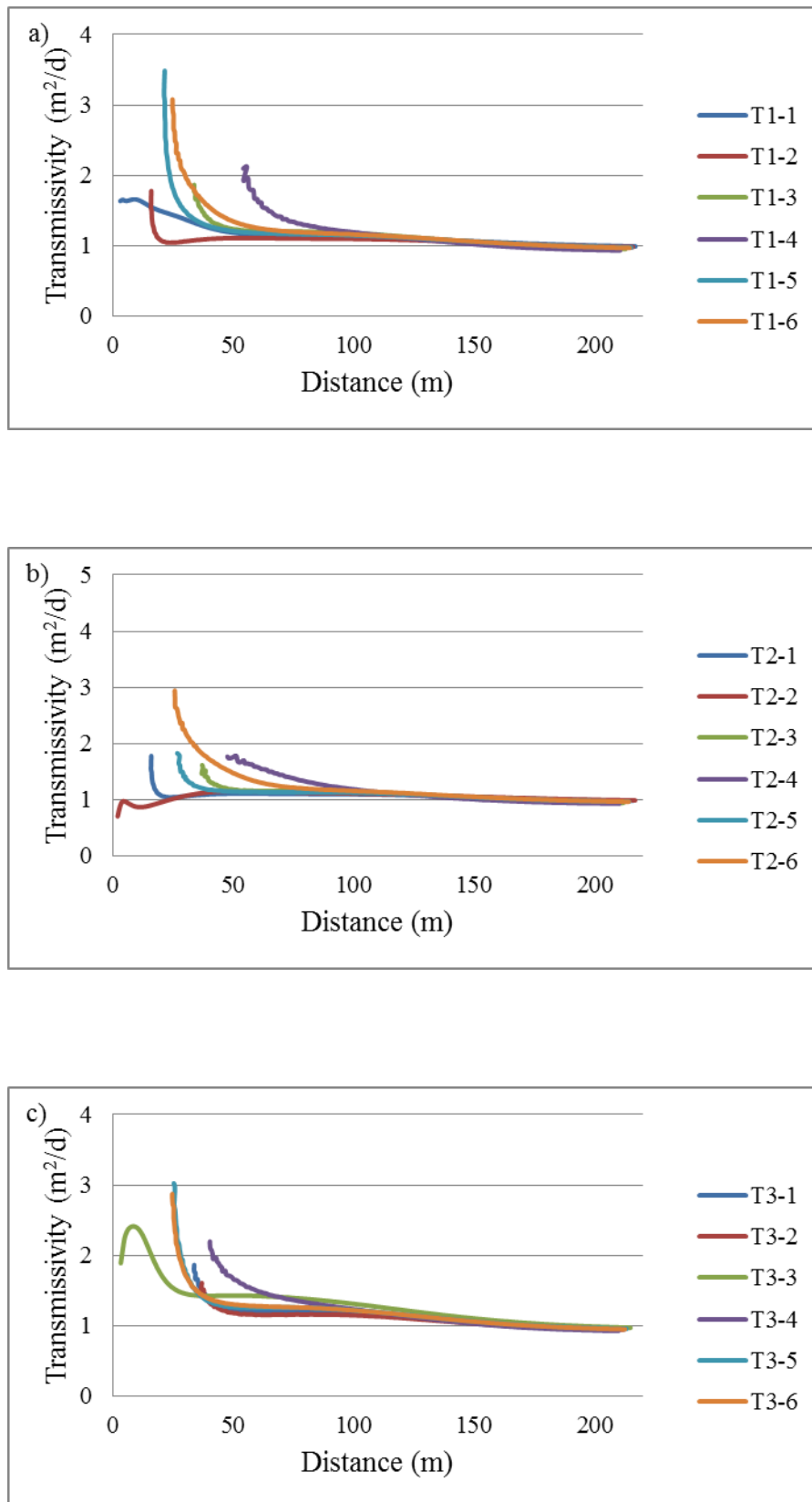


Figure 5.6. Transmissivity curves at each well for a) pumping test-1, b) pumping test-2, c) pumping test-3.

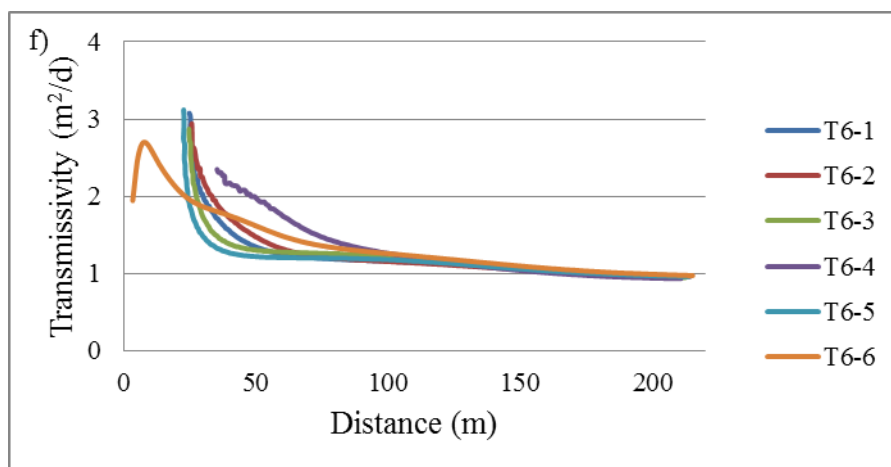
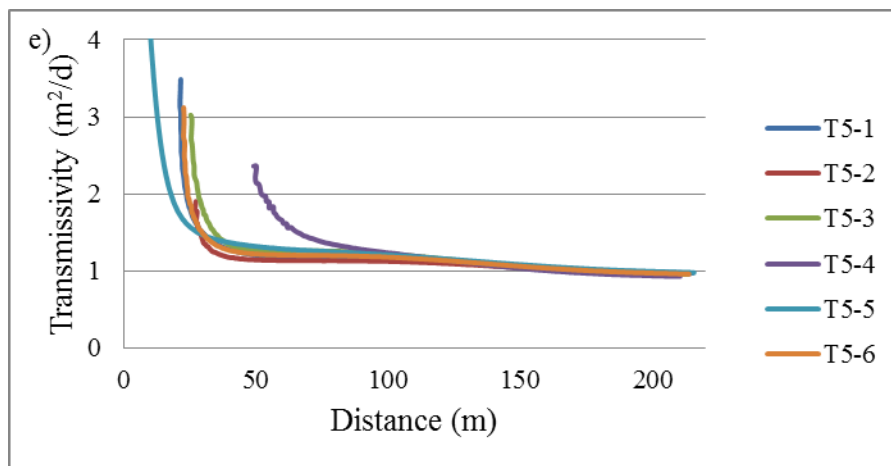
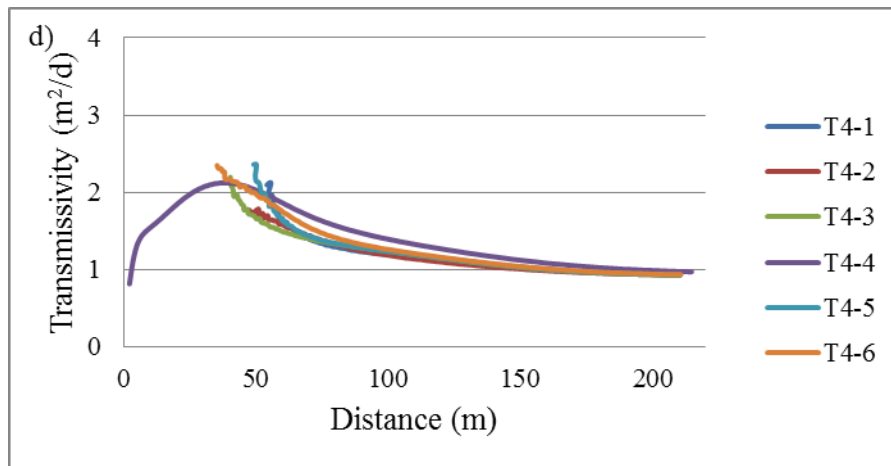


Figure 5.7. Transmissivity curves at each well for d) pinging test-4, e) pinging test-5, f) pumping test-6.

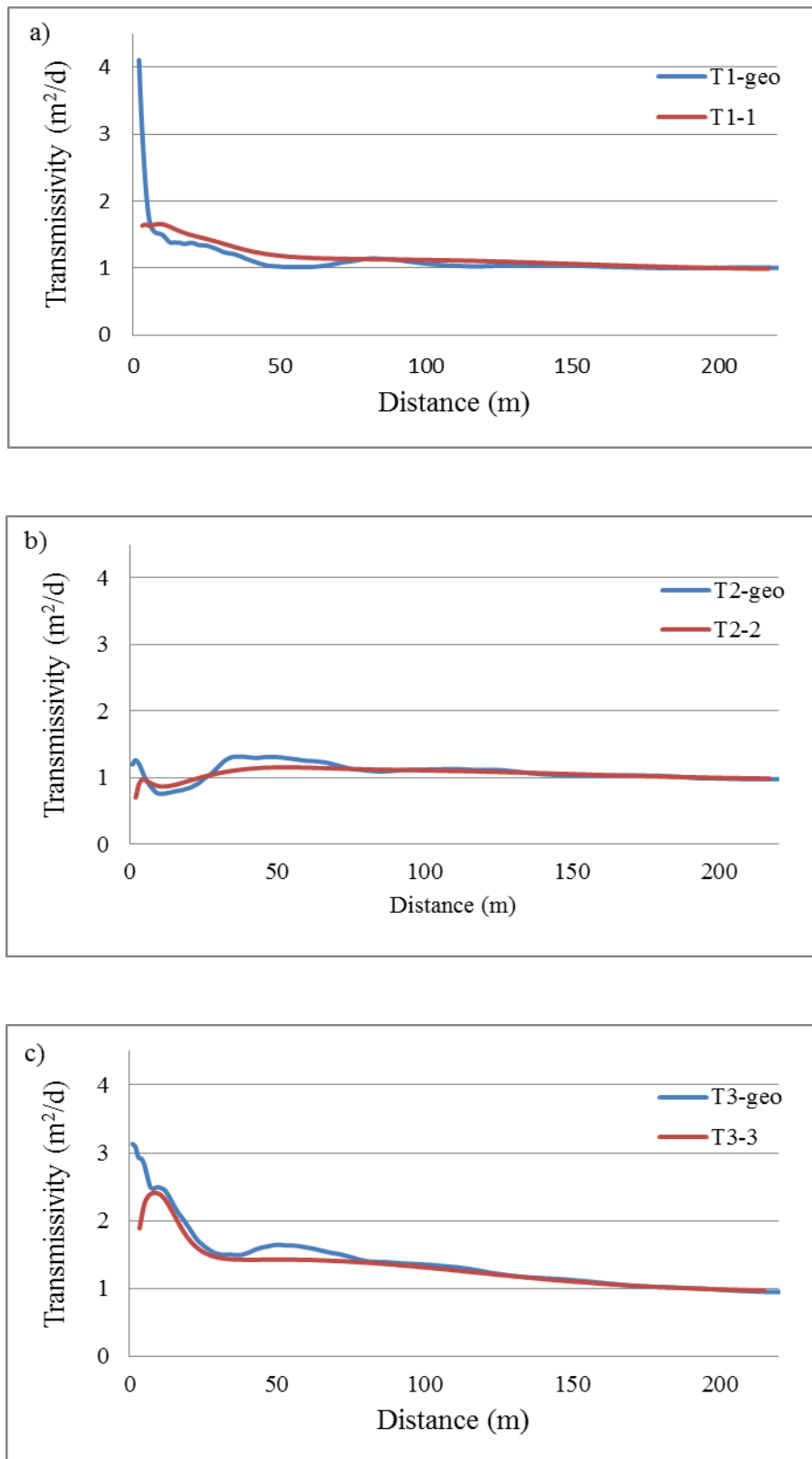


Figure 5.8. Estimated transmissivity using the continuous derivative method along with the geometric mean of the transmissivity as a function of radial distance from a) Well 1, b) Well 2, c) Well 3.

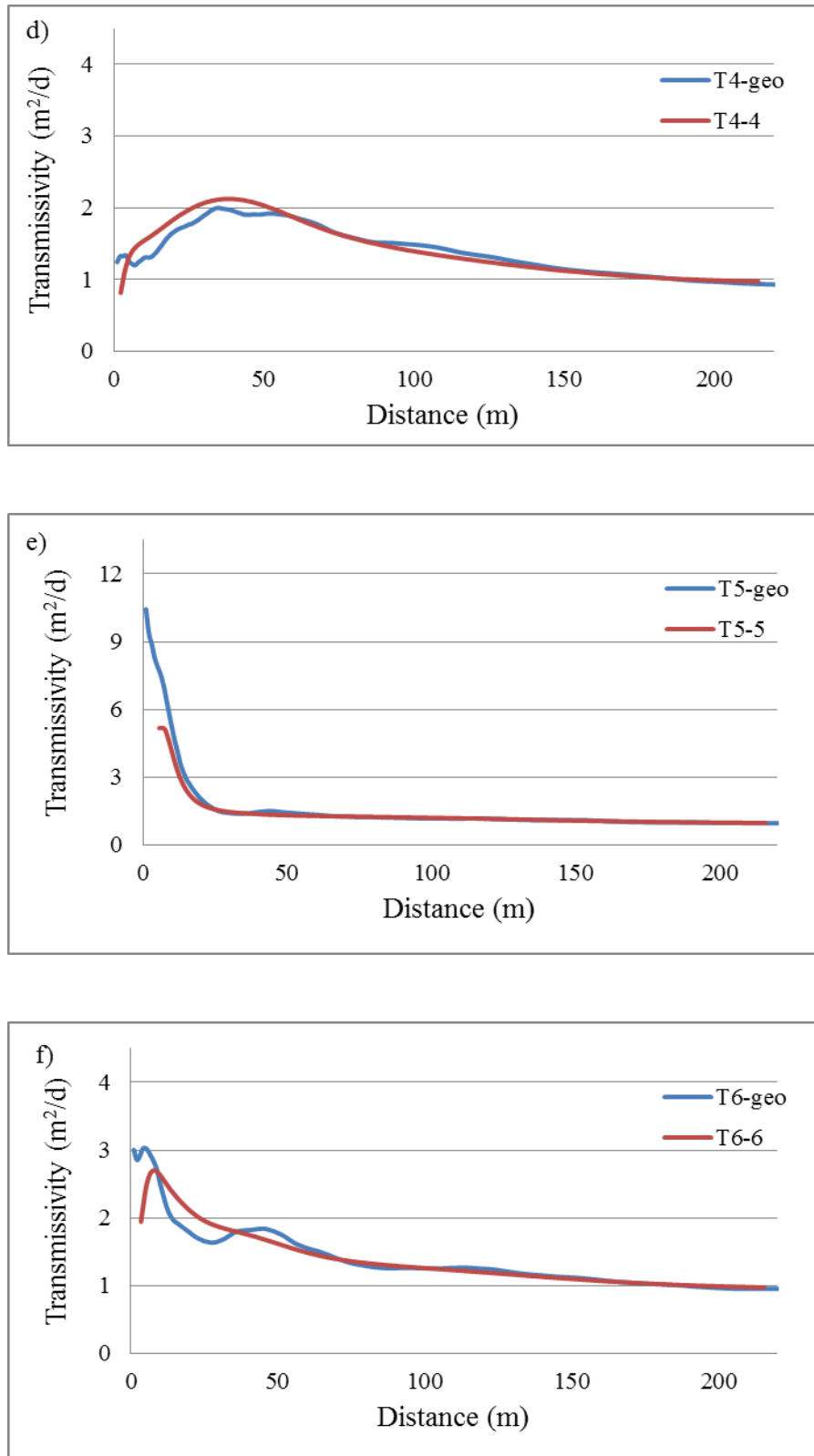


Figure 5.9. Estimated transmissivity using the continuous derivative method along with the geometric mean of the transmissivity as a function of radial distance from d) Well 4, e) Well 5, f) Well 6.

These results give an indication of how the transmissivity varies with distance as opposed to conventional methods such as the Theis and Cooper Jacob methods which provide only one “average” estimate of the transmissivity.

All curves tend to approach to 1, which is the geometric mean of the transmissivity used in the data generation. As it has been shown in previous studies, conventional methods tend to give estimates that are close to this mean value. Moreover, the curves show larger variability at the beginning of the tests because the early time data tend to reflect the conditions in the immediate vicinity of the pumping wells which may differ from one well to the other (Figure 5.6). At larger distances, the curves tend to approach to the mean transmissivity at a distance of about 10 to 20 integral scales which was used in the generation of the transmissivity data ($I=8$).

Figure 5.7 shows the estimated transmissivity at the pumping well which was obtained with the continuous derivation method along with the geometric mean of the transmissivity defined over a continuously increasing radial area centered at the pumping well. The agreement is quite significant suggesting that the transmissivity estimate obtained with the continuous derivation method is close to the geometric mean of the transmissivity field. For short distances from the well the variability is large because the geometric mean is defined over a small circular area (Figure 5.7). At larger distances, much larger than the integral scale of the transmissivity field, the average area would include many regions of high/low transmissivities, making the average close to the geometric mean.

This suggests that distance over which the estimated transmissivity approaches the geometric mean is indicative of the integral scale, while the variability of the estimated transmissivity near the pumping well is dependent on the variance of the transmissivity field (Figure 5.8). In the following section, two methods will be used to evaluate whether estimates of the integral scale and variance can be inferred from the pumping test data.

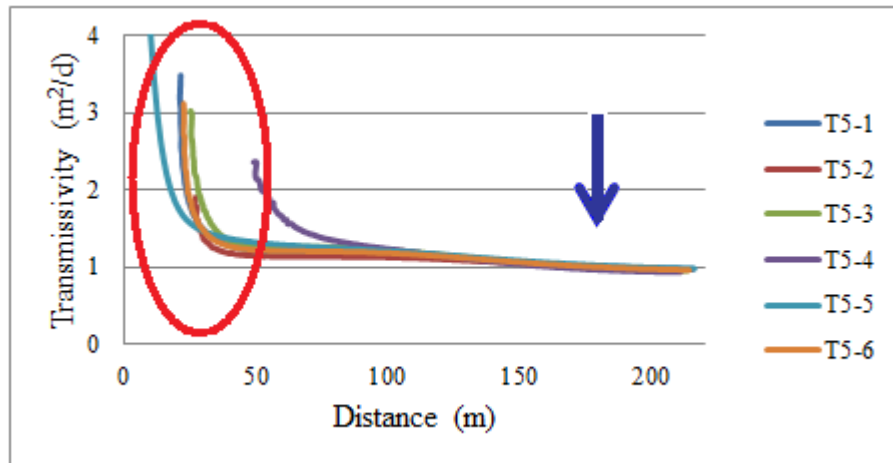


Figure 5.10. Estimation of statistical parameters, the variance and the integral scale, for the estimated transmissivity as a function of radial distance from the well.

5.3 The Estimation of Variance and Integral Scale

For the estimation of variance and integral scale, three sets of simulations were conducted:

- Set 1: mean, $m_y=0$; variance, $\sigma^2=1$; integral values, $I=8$.
- Set 2: mean, $m_y=0$; variance, $\sigma^2=2$; integral values, $I=8$.
- Set 3: mean, $m_y=0$; variance, $\sigma^2=1$; integral values, $I=24$.

For each set, 1000 transmissivity fields were generated. The transmissivity fields were then used as input to simulate the pumping test data as described in Section 4.4. Because of the large number of simulations, a slightly smaller domain was used (481 x 481 m). This however, does not affect the evaluation of the interpretation methods. Also, for each set, the integral scale and variance were estimated assuming $n=1$ (single pumping test), 5 and 10 pumping tests are available. The case of $n=5$ or 10 corresponds to hydraulic tomography with 5 and 10 wells, respectively.

In each case, the weighted least-squares approach and the Bayesian approach were used. The results of the weighted least-squares are presented below in Section 5.3.1 while the results of the Bayesian approach are presented in Section 5.3.2. Because each method is applied to a large number of realizations, the results will be presented in the form of a histogram of the estimated variance and integral scale which can be readily compared to the “actual” variance and integral scale values used in the transmissivity field generation.

With 3 sets of input parameters, 2 methods of estimation (the weighted least-squares approach and the Bayesian approach), 3 assumed number of pumping tests ($n=1, 5,$ and 10) and 2 parameters to estimate (variance and integral scale), the total number of histograms presented below is 36.

5.3.1 Weighted Least-Squares Method

Figure 5.9 to Figure 5.11 show the histograms of the estimated variance and integral scale corresponding to Set 1 transmissivity fields ($\sigma^2=1$ and $I=8$) and assuming $n=1, 5$ and 10 pumping test data are available, respectively. The parameters in each case were estimated using weighted least-squares. These results can be compared to the “actual” values used in the transmissivity generation, namely: $\sigma^2=1$ and $I=8$. The results indicate that the estimated variance agrees reasonably well with the “actual” value. The integral scale on the other hand appears to be more difficult to estimate reliably. For some realizations, the integral scale estimate is in good agreement with the actual value. However, for other realizations the estimate differs significantly. It is important however to note that the integral scale and the variance are statistical parameters that are defined over the entire domain. On the other hand, pumping tests provide information primarily about the region surrounding the pumping well. The difference between the estimated and actual values can be attributed to a large extent to the difference in the averaging volumes of the statistical parameters on one hand and the pumping tests on the other. As the number of pumping tests increases, the agreement between the estimated and actual parameters improves somewhat. To obtain good agreement for all realizations, a larger number of pumping tests, greater than $n=5$ or 10 which was considered in this study, would be

needed. This relates to the concept of ergodicity which basically states that the sample size must be large enough and with broad spatial coverage to represent the whole system (Kitanidis, 1997). Given the high costs of drilling wells, in practice it is not realistic to expect at most sites much larger number of wells than what was considered in this study.

The histograms obtained for Set 2 transmissivity fields ($\sigma^2=2$ and $I=8$) and $n=1, 5$ and 10 pumping tests are presented in Figures 5.12 to 5.14, respectively. When the $\ln T$ variance is increased to 2 (i.e., more heterogeneous fields) the estimation becomes more challenging because of the increased spatial variability. The increase in the number of pumping tests to $n=5$ and 10 did not result in significantly better variance estimation. On the other hand, some improvements in the integral scale estimation were obtained when the number of pumping tests increased. In particular, the number of realizations yielding integral scale estimates between $I=6$ and 10, (values close to the “actual” integral scale value, $I=8$) increased significantly with increase in n , the number of available pumping tests.

Figures 5.15 to 5.17 show the histograms corresponding to Set 3 transmissivity fields ($\sigma^2=1$ and $I=24$) and $n=1, 5$ and 10 pumping tests, respectively. When the $\ln T$ integral scale is increased to 24 which corresponds to a case of more gradual change in the transmissivity with distance, the estimation of the variance is reasonably good. Some improvement in the variance estimation is observed as the number of pumping tests increases. Narrower estimate distributions that are closer to the “actual” value are observed when the number of pumping tests increases. However, the estimation of the integral scale does not match well with the “actual” value.

Overall, the results presented in this section show that the weighted least-squares method can provide reasonable estimates of the variance particularly for the case of $\sigma^2=1$. The estimation does become more difficult when the variance increases and consequently the spatial variability of the transmissivity becomes more complex. On the other hand, the estimation of the integral scale with the least-squares method is more problematic. As indicated above, this is in part a result of the lack of ergodicity due to the relatively small number of pumping tests.

The lack of a good agreement between the estimated statistical parameters and the actual values is also due to the formulation of the weighted least-squares approach. The weighted least squares approach selects the best-fit estimates of the statistical parameters such that the estimated transmissivity versus distance is closest to the mean theoretical curves but excluding the spread around the mean that may exist. In contrast the Bayesian method, as will be discussed below, uses the entire probability density functions of the theoretical curves (please refer to Section 4.3.2).

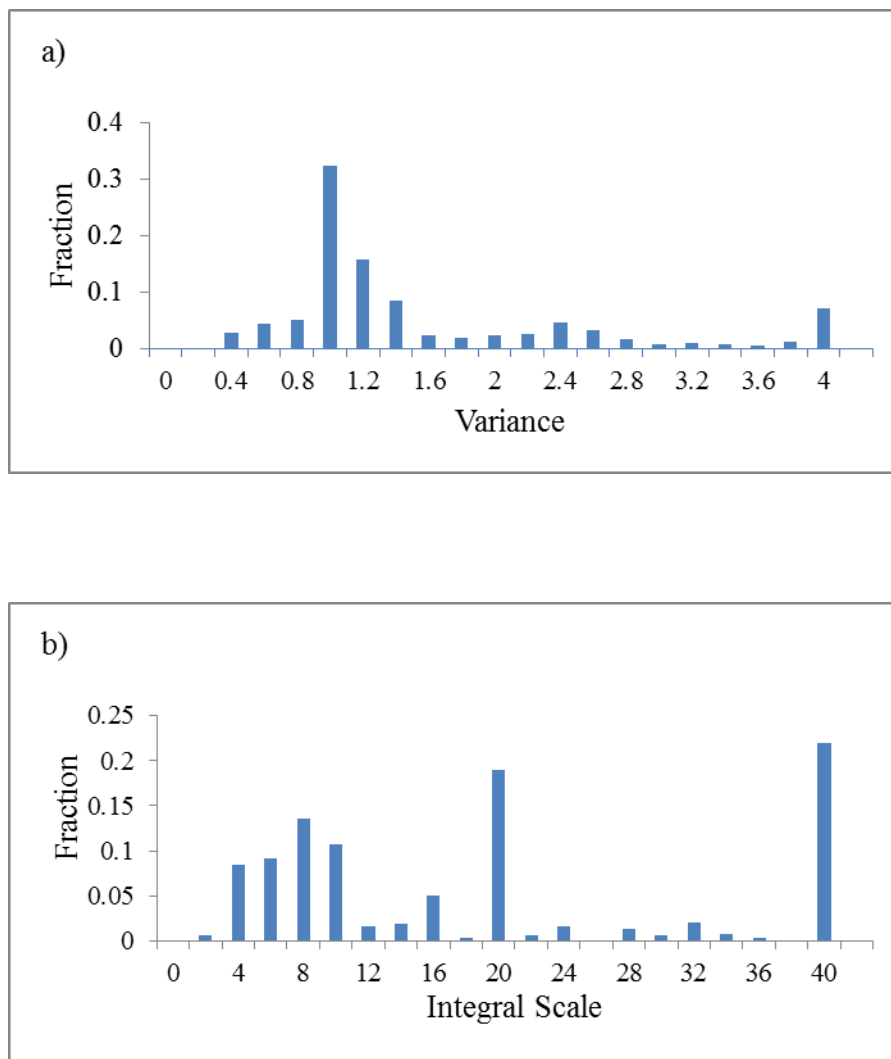


Figure 5.11. Histogram of (a) estimated variance and (b) estimated integral scale using weighted least-squares assuming $n=1$ pumping test is available for Set 1 transmissivity fields ($\sigma^2=1$ and $I=8$).

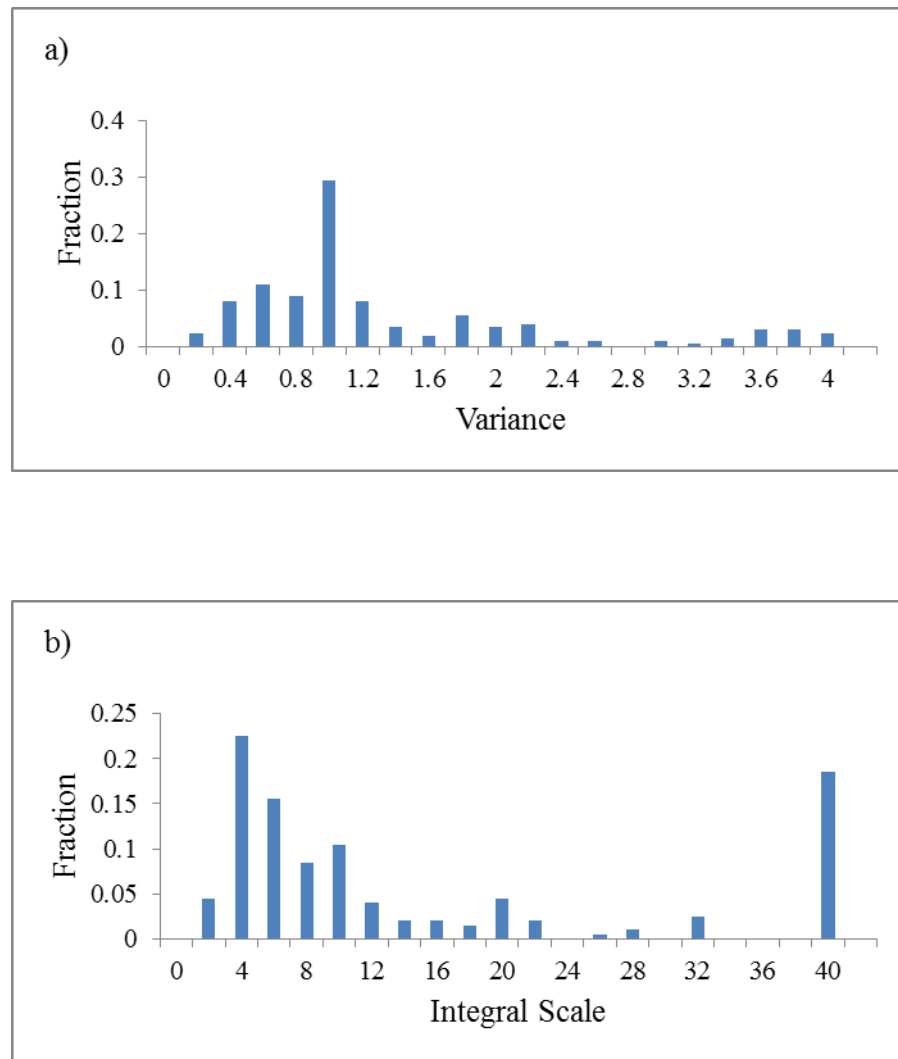


Figure 5.12. Histogram of (a) estimated variance and (b) estimated integral scale using weighted least-squares assuming $n=5$ pumping test is available for Set 1 transmissivity fields ($\sigma^2=1$ and $I=8$).

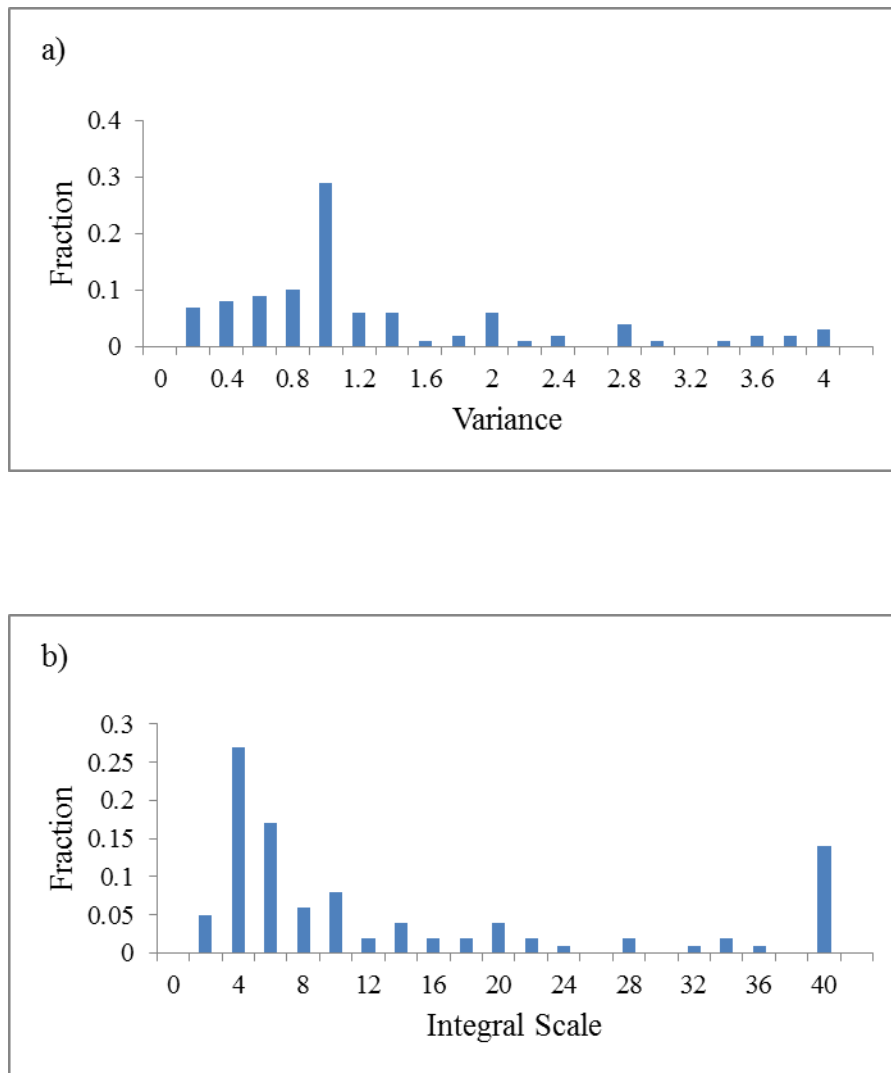


Figure 5.13. Histogram of (a) estimated variance and (b) estimated integral scale using weighted least-squares assuming $n=10$ pumping test is available for Set 1 transmissivity fields ($\sigma^2=1$ and $I=8$).

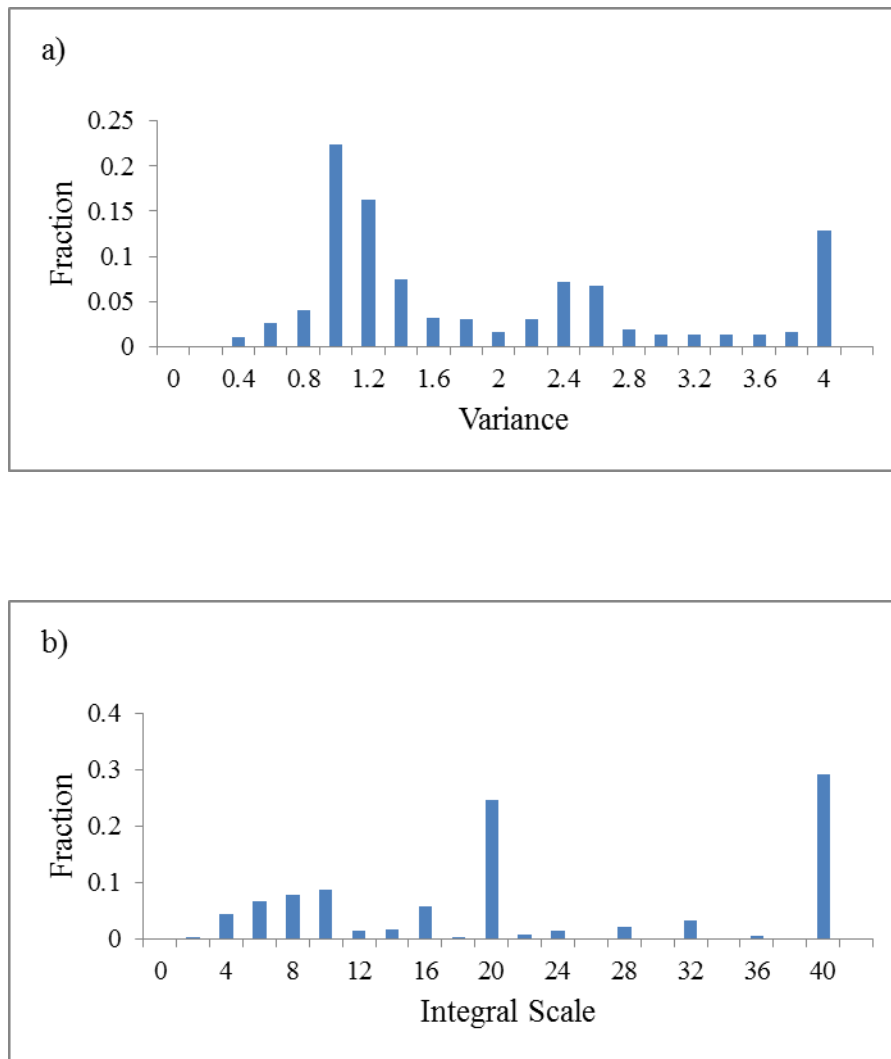


Figure 5.14. Histogram of (a) estimated variance and (b) estimated integral scale using weighted least-squares assuming $n=1$ pumping test is available for Set 2 transmissivity fields ($\sigma^2=2$ and $I=8$).

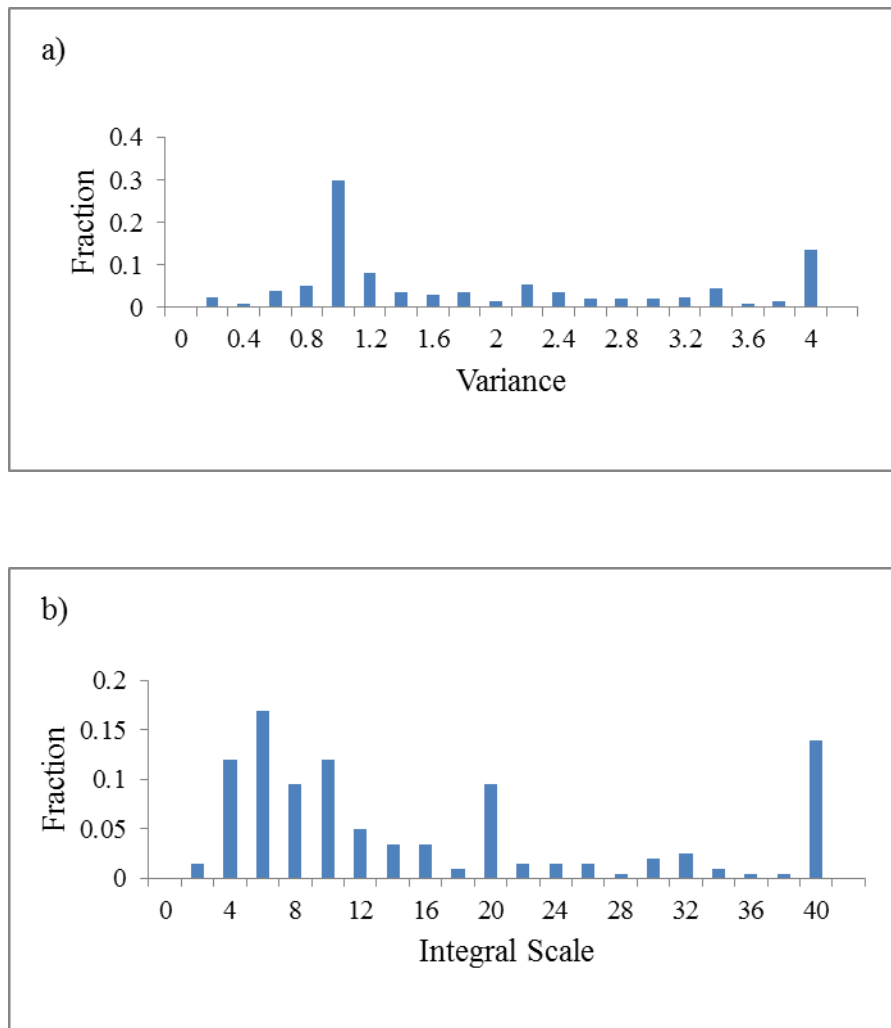


Figure 5.15. Histogram of (a) estimated variance and (b) estimated integral scale using weighted least-squares assuming $n=5$ pumping test is available for Set 2 transmissivity fields ($\sigma^2=2$ and $I=8$).

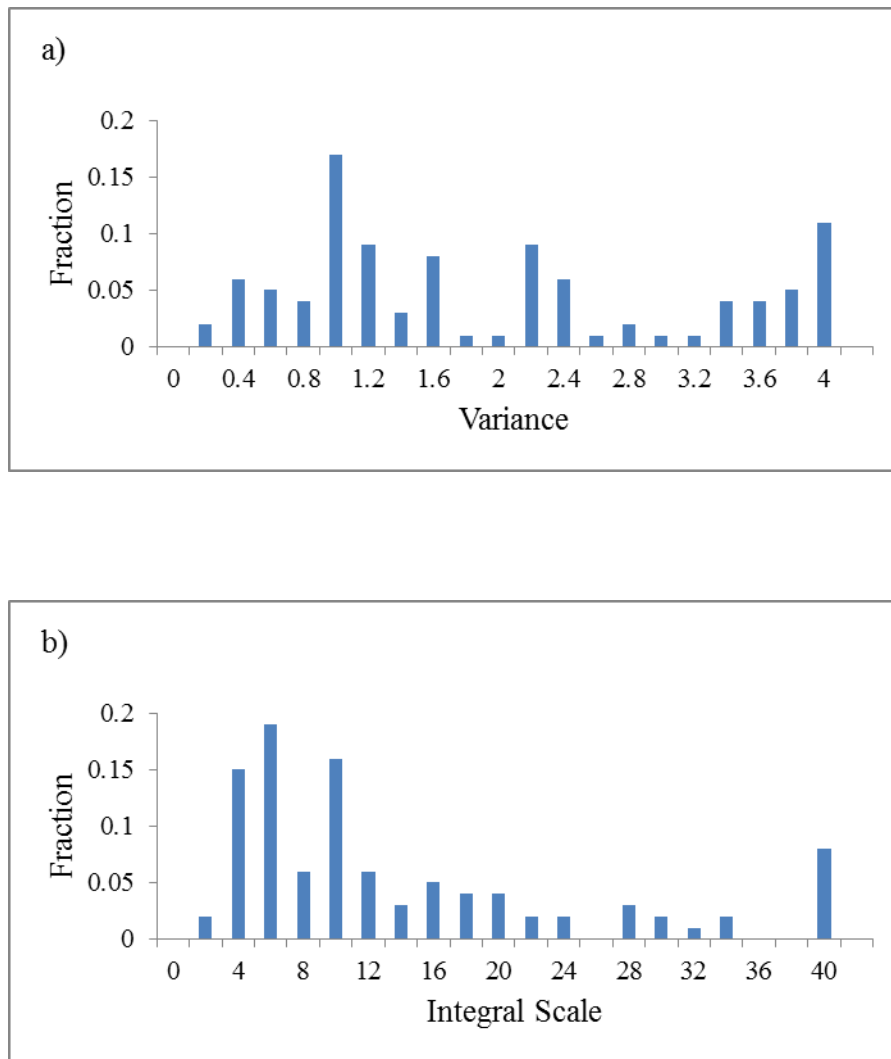


Figure 5.16. Histogram of (a) estimated variance and (b) estimated integral scale using weighted least-squares assuming $n=10$ pumping test is available for Set 2 transmissivity fields ($\sigma^2=2$ and $I=8$).

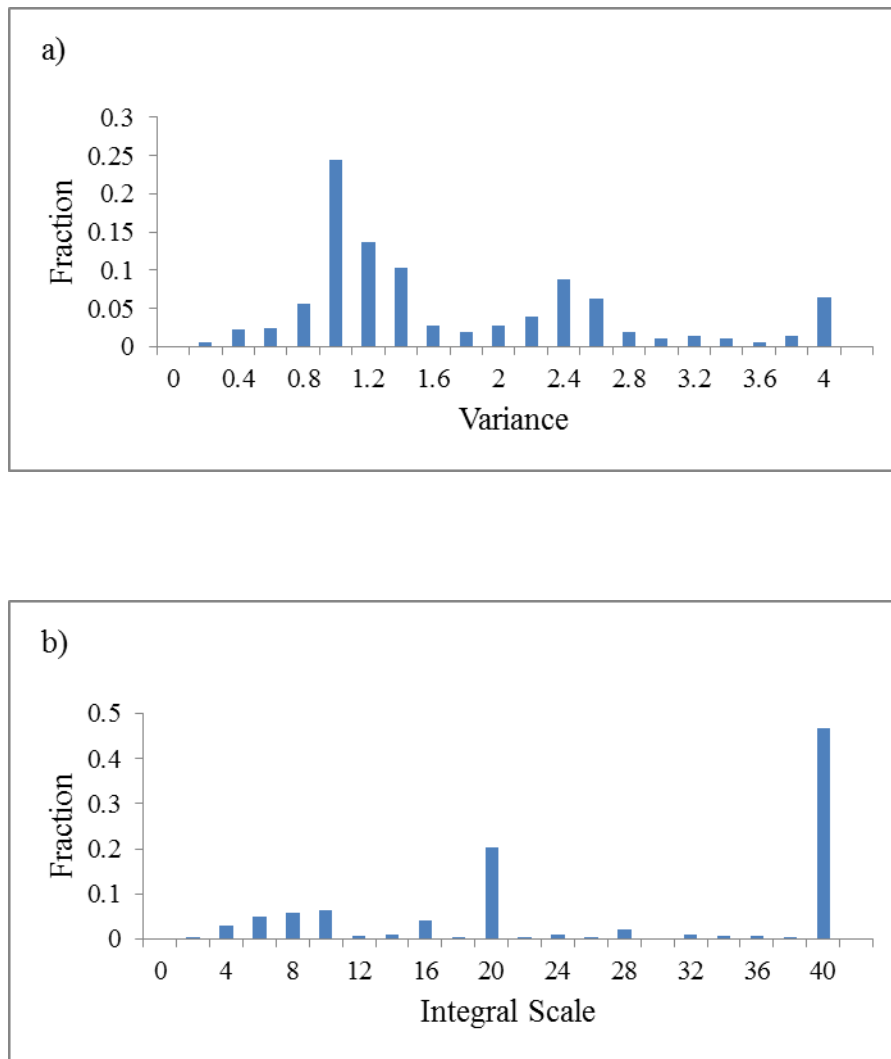


Figure 5.17. Histogram of (a) estimated variance and (b) estimated integral scale using weighted least-squares assuming $n=1$ pumping test is available for Set 3 transmissivity fields ($\sigma^2=1$ and $I=24$).

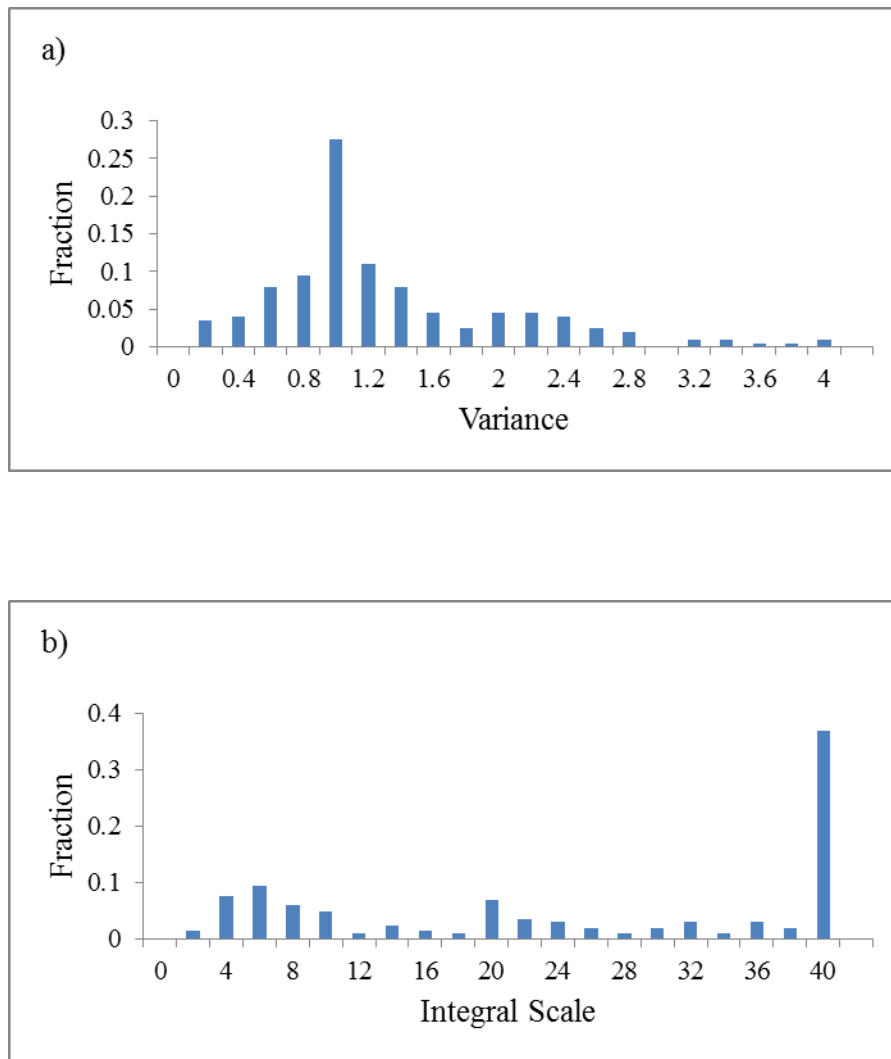


Figure 5.18. Histogram of (a) estimated variance and (b) estimated integral scale using weighted least-squares assuming $n=5$ pumping test is available for Set 3 transmissivity fields ($\sigma^2=1$ and $I=24$).

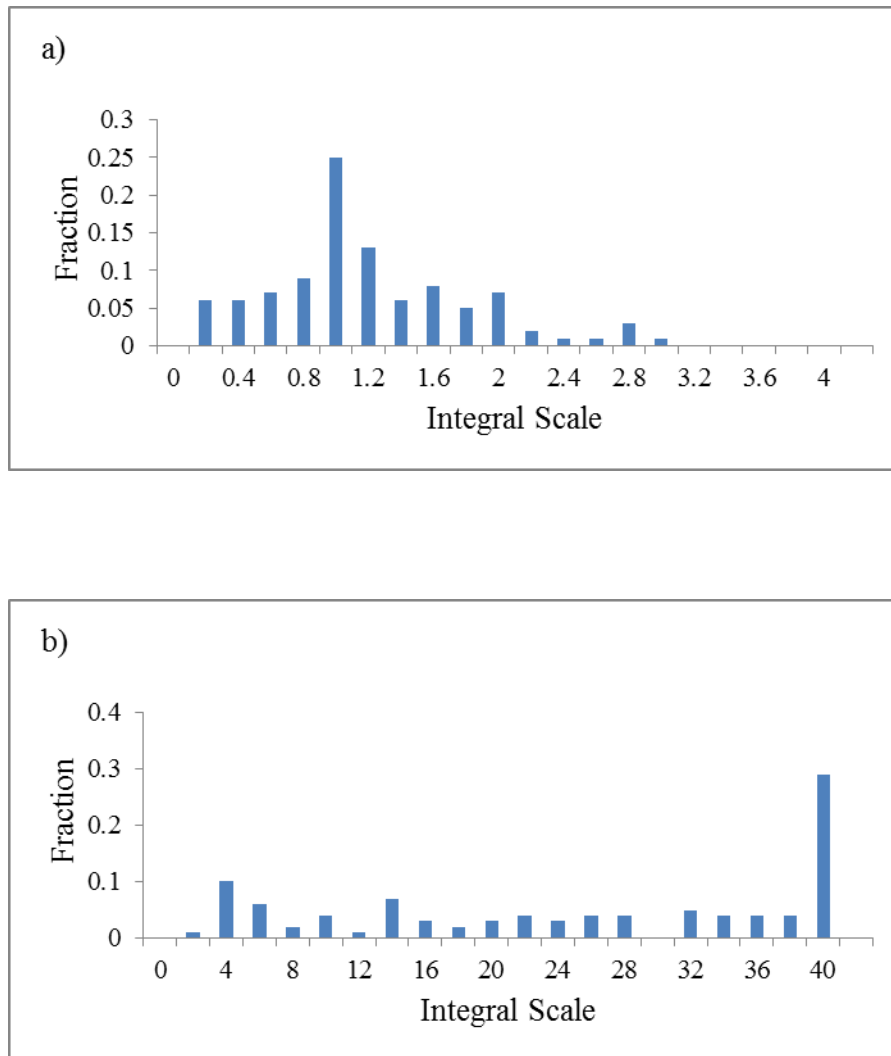


Figure 5.19. Histogram of (a) estimated variance and (b) estimated integral scale using weighted least-squares assuming $n=10$ pumping test is available for Set 3 transmissivity fields ($\sigma^2=1$ and $I=24$).

5.3.1 Bayesian Method

The Bayesian estimation requires the definition of a “prior” or an initial distribution for the estimates before accounting for the pumping test data. The pumping test data will then be used, along with the prior distribution, to estimate a posterior distribution that takes into account both sources of information the prior and the pumping tests. In our case, we have assumed minimum prior information consisting of a uniform distribution between 0 and 4 for the variance and a uniform distribution between 0 and 40 for the integral scale. The expected values of these two prior distributions are 2 and 20, respectively.

When the pumping test data are included, we see a shift in the estimated variance and integral scale towards the true values ($\sigma^2=1$ and $I=8$ for Set 1, $\sigma^2=2$ and $I=8$ for Set 2, $\sigma^2=1$ and $I=24$ for Set 3). However, the impact of the prior remains evident in the estimated histograms.

Figure 5.18 to Figure 5.20 show the histogram of the estimated variance and integral scale corresponding to Set 1 transmissivity fields ($\sigma^2=1$ and $I=8$) and assuming $n=1, 5$ and 10 pumping test data are available, respectively. These results can be compared to the “actual” values used in the transmissivity generation, namely: $\sigma^2=1$ and $I=8$. The results show that the estimation of variance is considerably close to the “actual” value. The Bayesian method can be considered as a weighted average of the prior probability density function and the results of the pumping test. In Figures 5.18 to 5.20, conditioning the prior distributions to the pumping test data results in a shift towards the “actual” parameter values. Moreover, these results were enhanced with the increase in the number of available pumping tests. The integral scale, however, appears to be under the strong influence of the prior distributions although the increase in number of pumping tests, n , from 1 to 5 and 10 created a little shift towards the actual value. This suggests that the pumping test data do not reveal much information about the integral scale and, as a result, the posterior distribution is close to the prior distribution.

The histograms obtained for Set 2 transmissivity fields ($\sigma^2=2$ and $I=8$) and $n=1, 5$ and 10 pumping tests are shown in Figures 5.21 to 5.23. Because of the increased spatial

variability, the estimation becomes more difficult. Some shift toward to the “actual” values of variance and integral scale were observed in the histograms. The increase in the number of pumping tests displays a slight change in the posterior distribution towards the actual values. In the case of Set 1, a larger shift from the prior estimate towards the actual value is observed compared to Set 2. However, generally, the results remain dependent on the prior distribution reflecting the wide spread in the probability density functions of the theoretical curves.

Figures 5.24 to 5.26 demonstrate the histograms corresponding to Set 3 transmissivity fields ($\sigma^2=1$ and $I=24$) and $n=1, 5$ and 10 pumping tests, respectively. As in the case of Set 1, the estimation of variance is acceptably good. Because the “actual” value of integral scale is very close to the prior estimation of it, the results of integral scale estimation of Set 3 are also satisfactory. Moreover, the increase in the number of pumping tests makes the distribution of both the variance and integral scale narrower and therefore associated with less uncertainty.

In comparison to the weighted least-squares approach, the Bayesian approach yielded on the whole better results that are closer to the “actual” values used in data generation. The weighted least-squares method selects the best-fit estimates based on a comparison of the transmissivity estimates from the pumping test and average theoretical curves. The Bayesian formulation on the other hand has a number of attractive features that do not exist in the least-squares formulation. First, it allows for the incorporation of previous information about the site in the form of a prior distribution. Second, the uncertainty in the prior as well as the pumping test data is accounted for. The prior and the pumping test data are combined together to yield a posterior distribution that is dependent on all available data. Third, the current posterior distribution can act as the prior distribution if additional tests are conducted in the future.

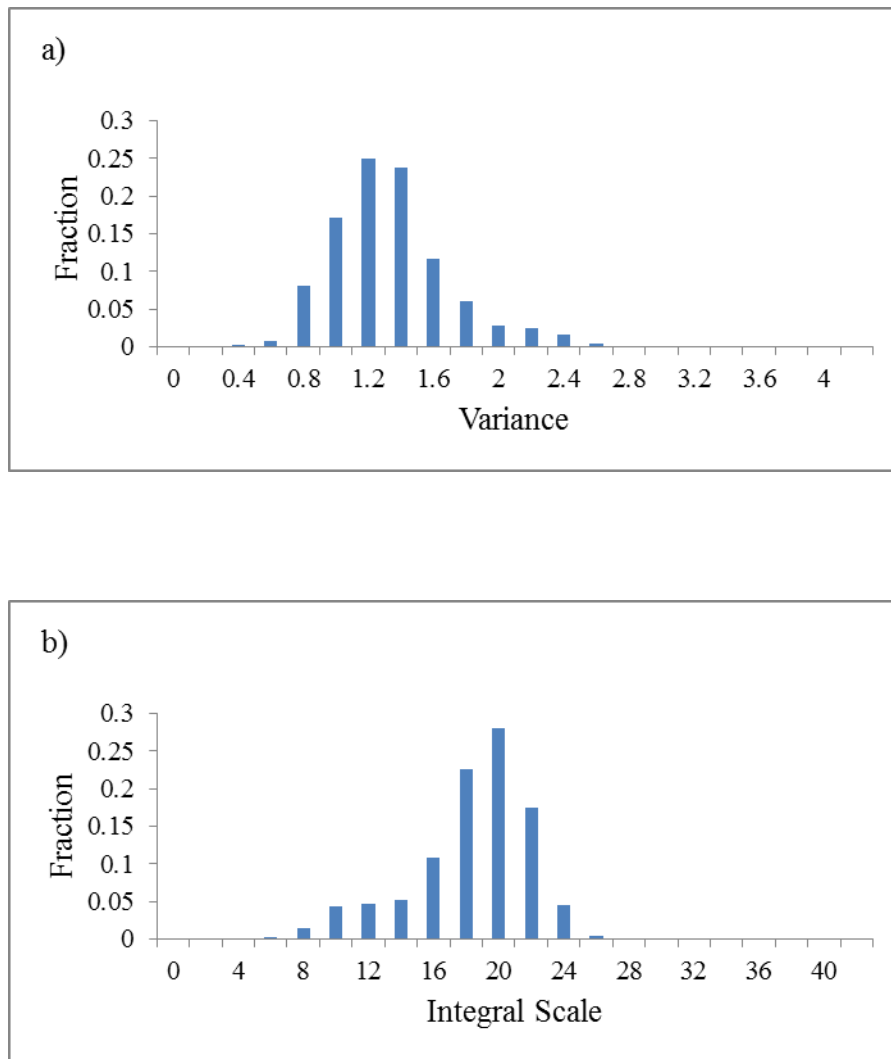


Figure 5.20. Histogram of (a) estimated variance and (b) estimated integral scale using Bayesian method assuming $n=1$ pumping test is available for Set 1 transmissivity fields ($\sigma^2=1$ and $I=8$).

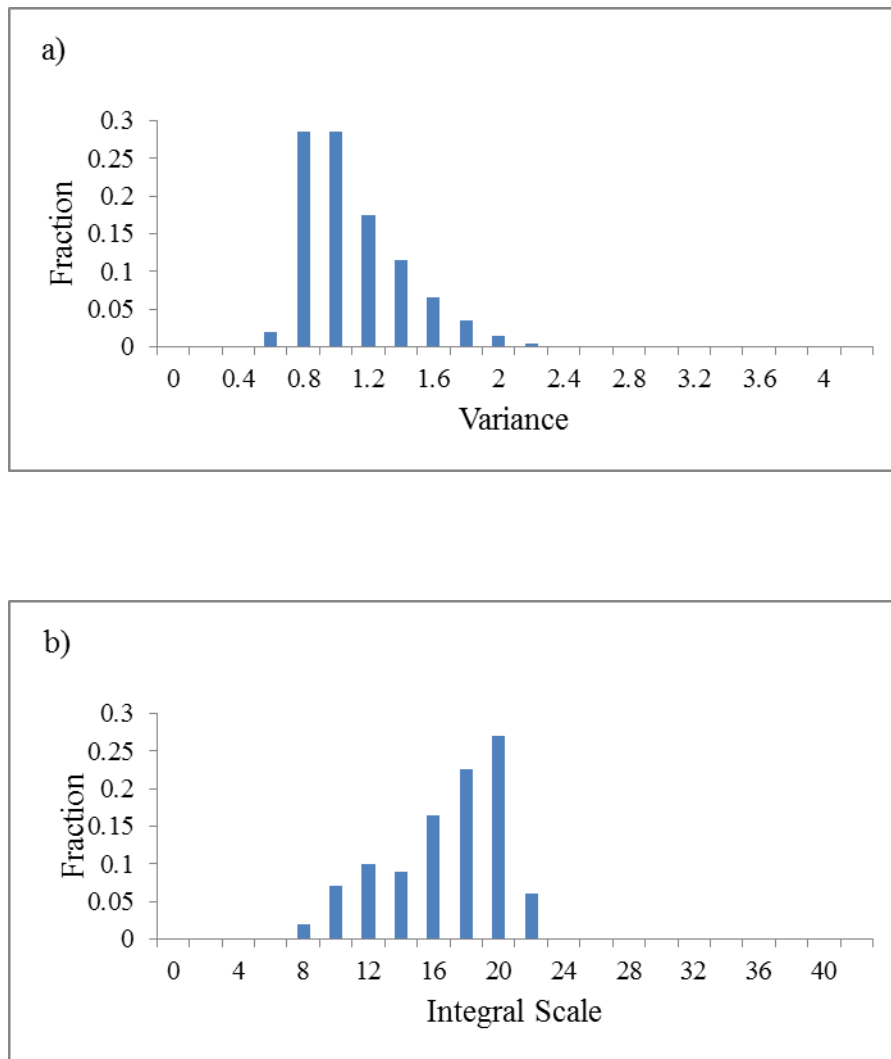


Figure 5.21. Histogram of (a) estimated variance and (b) estimated integral scale using Bayesian method assuming $n=5$ pumping test is available for Set 1 transmissivity fields ($\sigma^2=1$ and $I=8$).

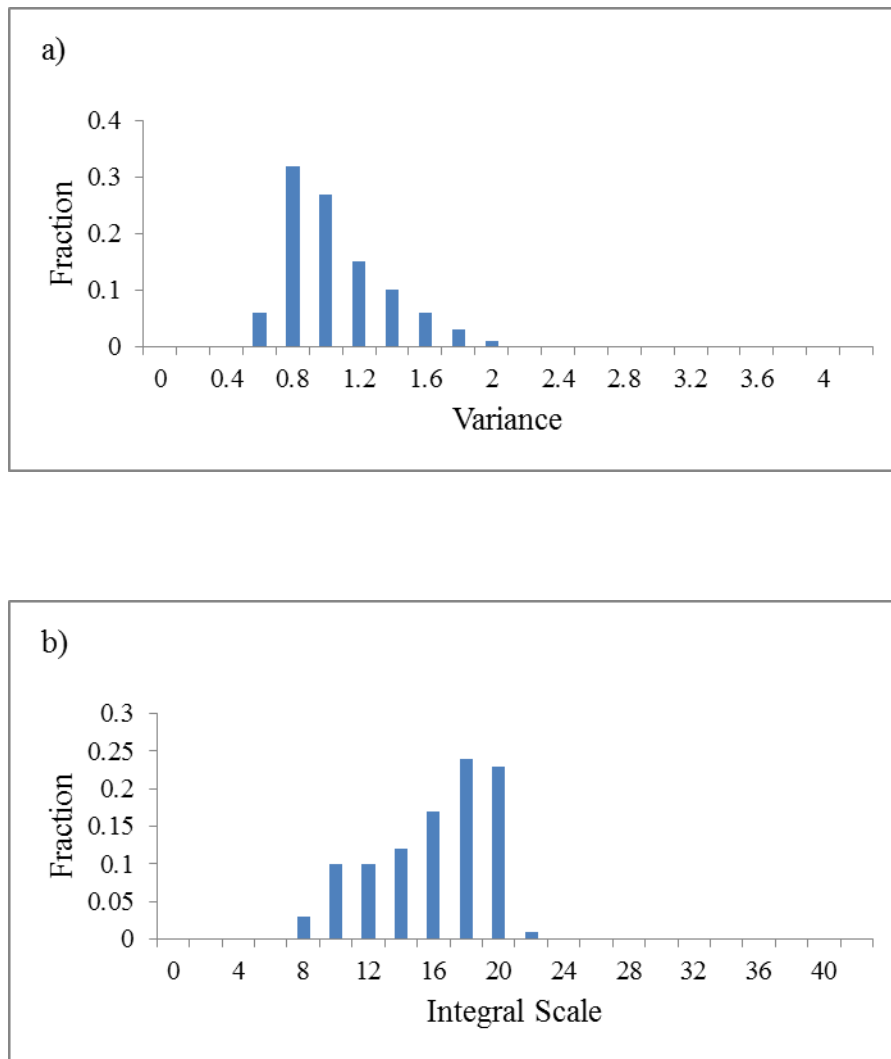


Figure 5.22. Histogram of (a) estimated variance and (b) estimated integral scale using Bayesian method assuming $n=10$ pumping test is available for Set 1 transmissivity fields ($\sigma^2=1$ and $I=8$).

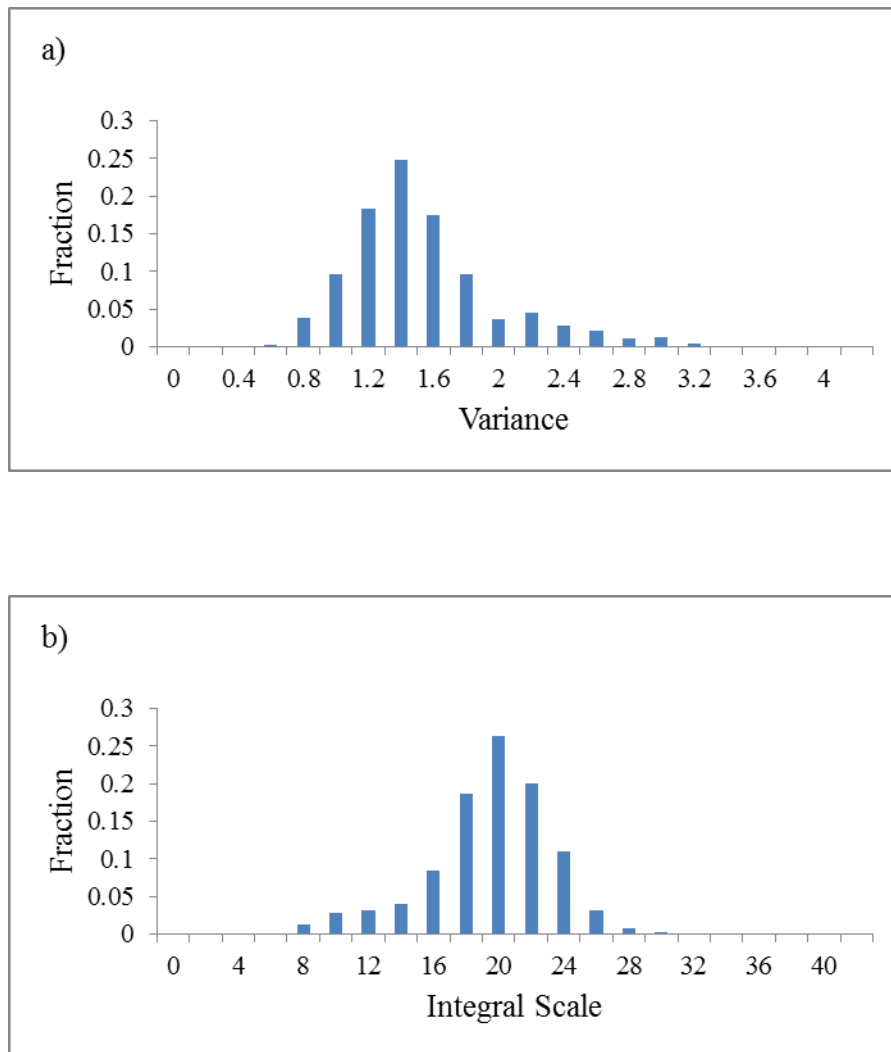


Figure 5.23. Histogram of (a) estimated variance and (b) estimated integral scale using Bayesian method assuming $n=1$ pumping test is available for Set 2 transmissivity fields ($\sigma^2=2$ and $I=8$).

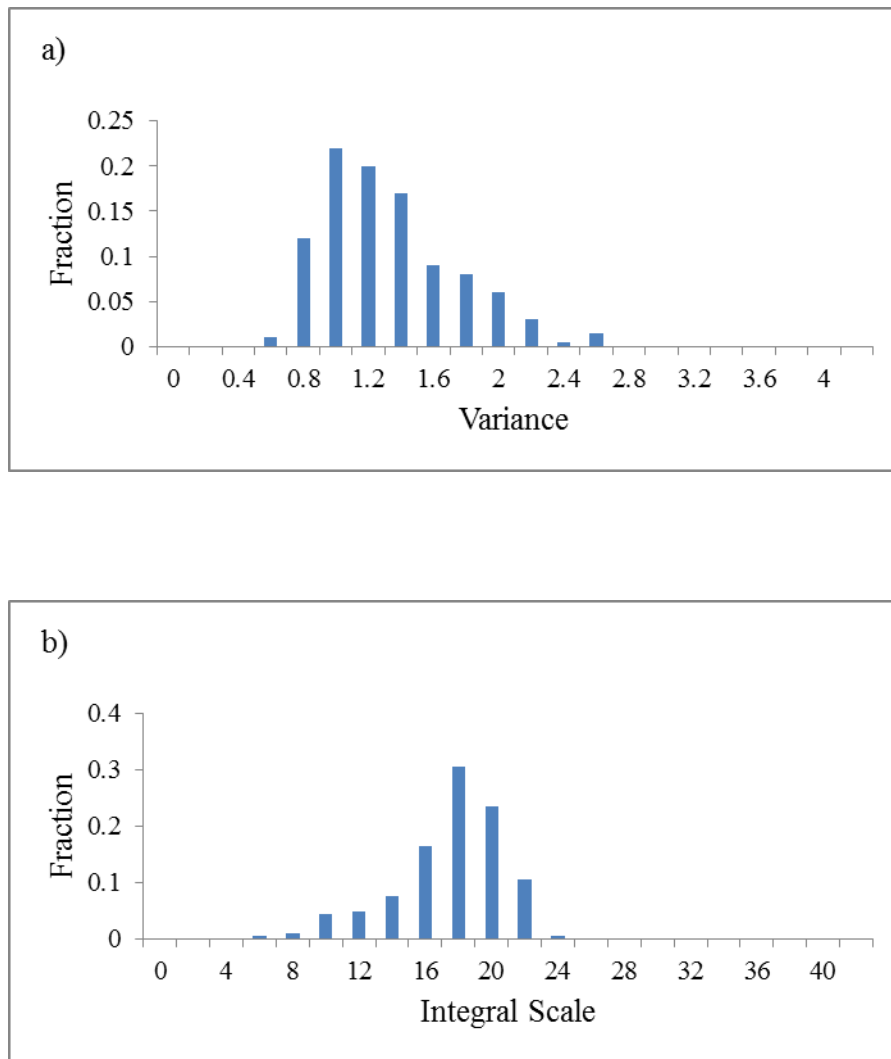


Figure 5.24. Histogram of (a) estimated variance and (b) estimated integral scale using Bayesian method assuming $n=5$ pumping test is available for Set 2 transmissivity fields ($\sigma^2=2$ and $I=8$).

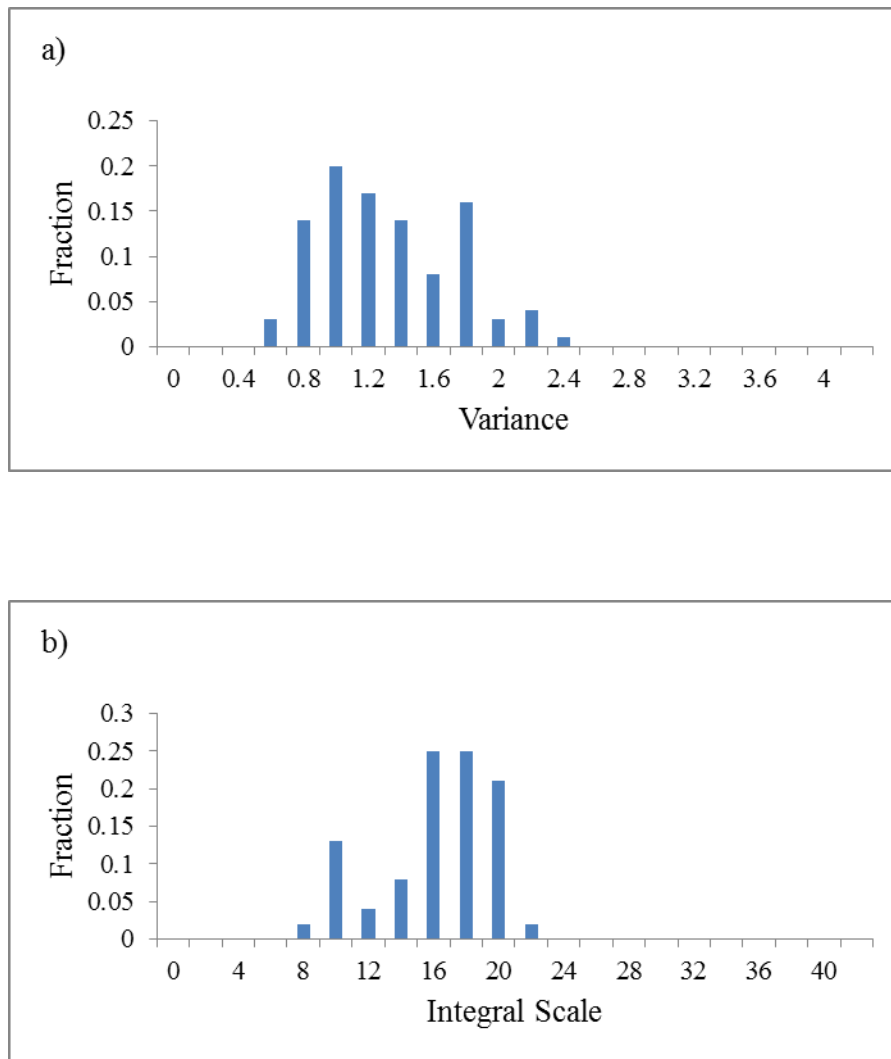


Figure 5.25. Histogram of (a) estimated variance and (b) estimated integral scale using Bayesian method assuming $n=10$ pumping test is available for Set 2 transmissivity fields ($\sigma^2=2$ and $I=8$).

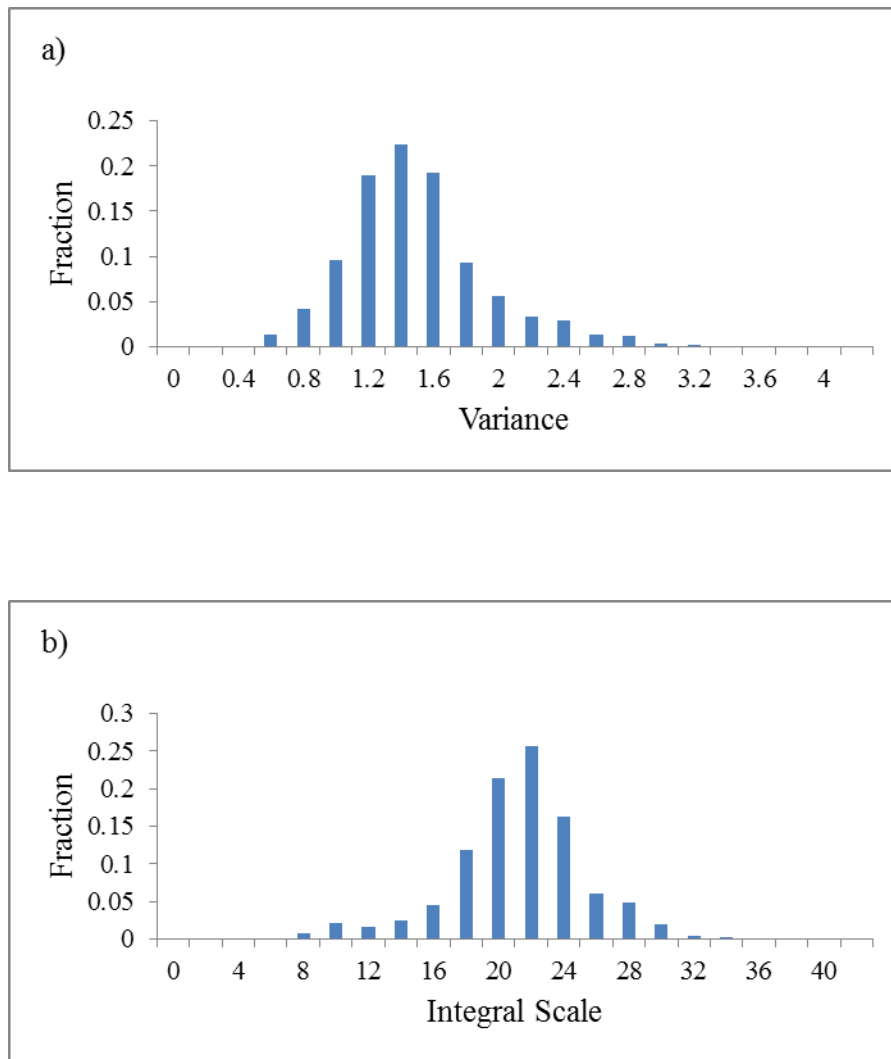


Figure 5.26. Histogram of (a) estimated variance and (b) estimated integral scale using Bayesian method assuming $n=1$ pumping test is available for Set 3 transmissivity fields ($\sigma^2=1$ and $I=24$).

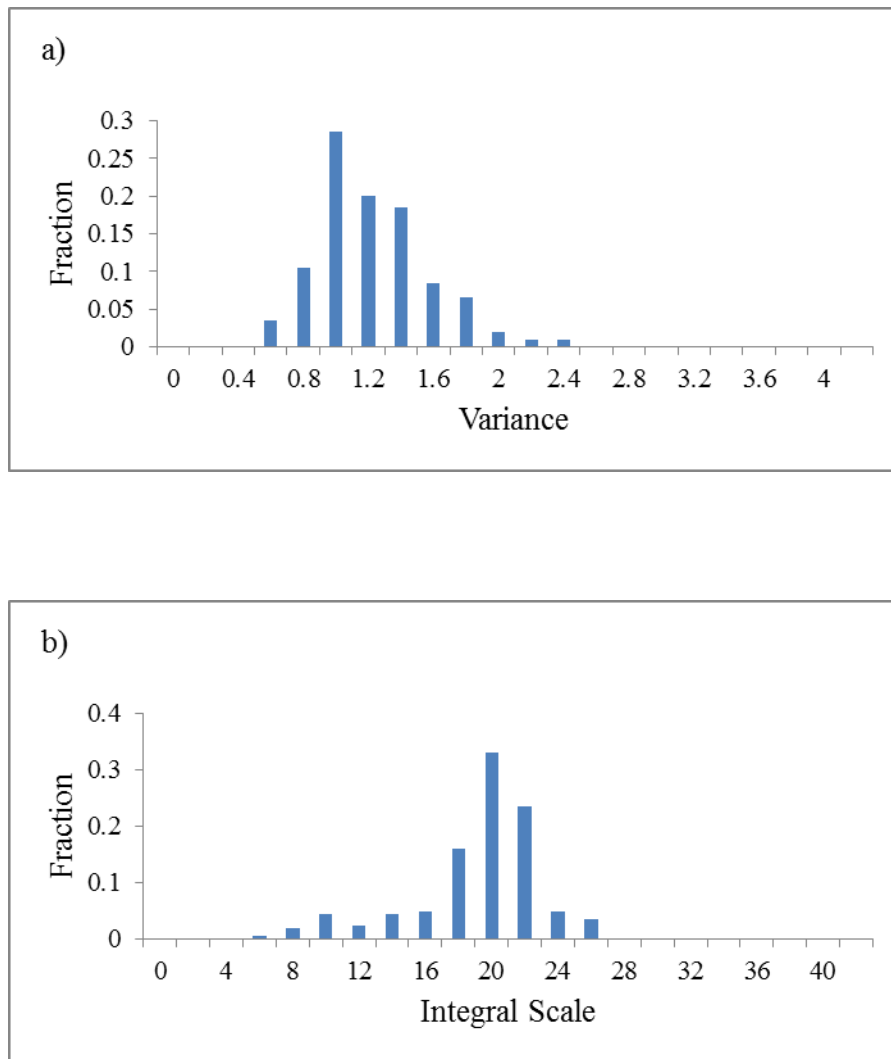


Figure 5.27. Histogram of (a) estimated variance and (b) estimated integral scale using Bayesian method assuming $n=5$ pumping test is available for Set 3 transmissivity fields ($\sigma^2=1$ and $I=24$).

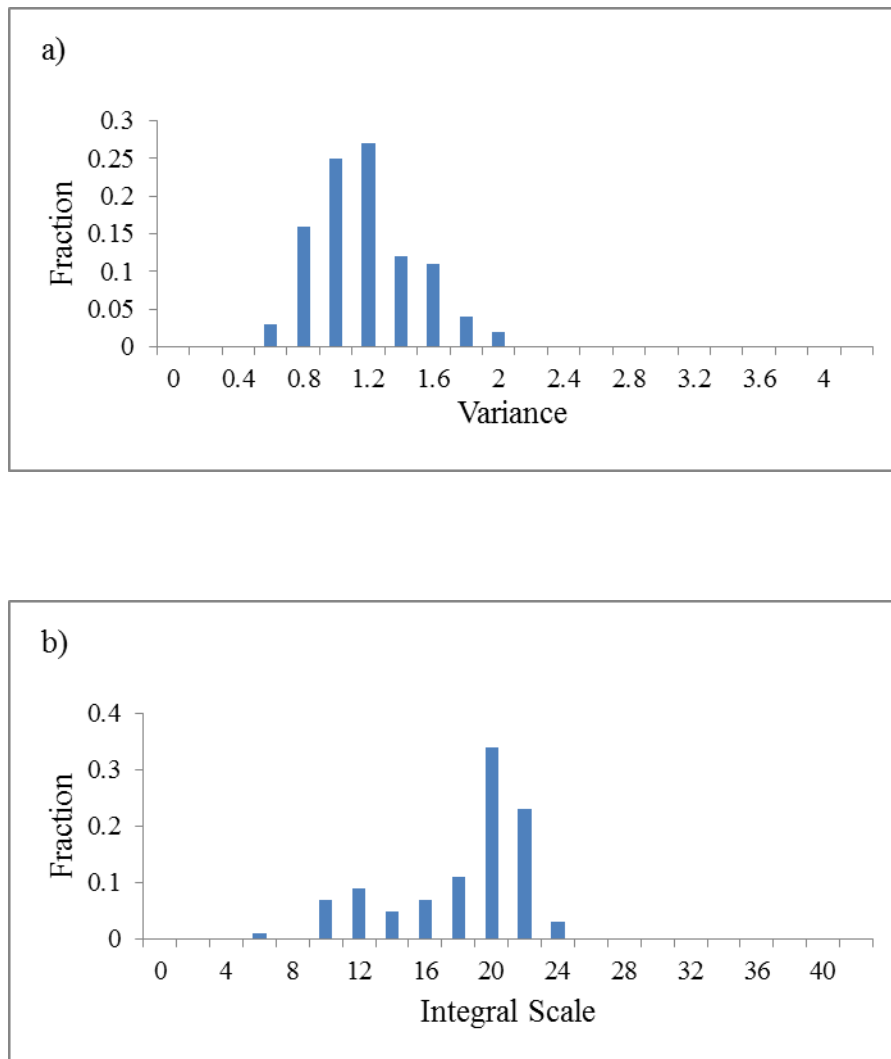


Figure 5.28. Histogram of (a) estimated variance and (b) estimated integral scale using Bayesian method assuming $n=10$ pumping test is available for Set 3 transmissivity fields ($\sigma^2=1$ and $I=24$).

6. CONCLUSIONS AND RECOMMENDATIONS

Groundwater flow and contaminant transport is strongly influenced by the heterogeneity of subsurface systems. The heterogeneity of the subsurface structure manifests itself as large and complex spatial variations in the groundwater flow parameters. This spatial variability of the flow parameters has a fundamental role on the infiltration, transport and storage of the groundwater as well as the transport of contaminants in groundwater. Therefore, the estimation of the spatial variability of groundwater flow parameters is a must for the groundwater flow and contaminant transport processes.

The purpose of this study is to expand a recently developed pumping test interpretation method, the Continuous Derivation method (Copty et al., 2011), which uses the drawdown and its time derivative for the estimation of more detailed information about the spatial variability of the flow parameters, with data gained from hydraulic tomography. In particular, the main goal was to estimate the variance and integral scale parameters of the transmissivity field. This is in contrast to conventional methods which are based on the assumption of homogeneity and hence attempt to estimate single representative values of the transmissivity. Single well as well as multiple pumping test data were considered in this study. Moreover, the effect of the available number of wells was also investigated. In order to estimate the parameters of the statistical spatial structure, (integral scale and variance) two approaches were considered: a weighted least-squares approach and a Bayesian approach.

The results of the study show that the weighted least-squares approach tends to pick the best-fit estimates by comparing the estimated transmissivity curves with the averaged theoretical curves. On the other hand, Bayesian method can be seen as a weighted average of the entire prior probability density function and the results of the pumping test. To better assess the robustness of the pumping test interpretation methods, the analysis was repeated for different statistical parameter values and for a large number of simulations.

The application of the continuous derivation method to the pumping test data shows that the estimated transmissivity is close to the geometric mean of the transmissivity field as a function of radial distance from the pumping well. At early times, the estimated transmissivity is close to the transmissivity at the well. At later times, the transmissivity is close to the geometric average of a much larger aquifer volume. Analysis of the estimated transmissivity function suggested that the early part of the curve is sensitive to the variance of the transmissivity field while the rate of convergence towards the spatial mean of the domain is mostly function of the integral scale. This provides some basis for attempting to estimate the variance and integral scale of the transmissivity field from the pumping test data.

The results of this study also show that the estimation of variance by using the weighted least-squares is acceptable, while the estimation of integral scale is more challenging. The increase in the number of pumping tests results in improved agreement between the estimated and actual parameters. In order to get better estimates of variance and integral scale for all realizations, larger number of pumping tests than the number of pumping tests considered in this study is necessary. This situation can be related to the lack of ergodicity due to the insufficient number of pumping tests to fully represent the entire flow domain.

On the other hand, more reliable results were obtained with the Bayesian approach. In other words, the results of the Bayesian approach yielded closer estimates to “actual” values of the generated fields. Also, the results of Bayesian approach improved with the increase in the number of available pumping tests. A main feature of the Bayesian approach is that it accounts for the uncertainty of the associated with the statistical parameters which can be significant particularly when the data are scarce.

Overall, the findings of this study highlight the difficulty of solving the inverse problem, namely the estimation of representative parameter values from observed data. The challenges of this problem stem from the non-uniqueness of the inverse problem, meaning the presence of more than one set of parameters that can yield the same observations. This is particularly true when data are scarce.

Possible avenues for future research include:

- The focus in this study was on confined aquifers. Future research can consider other types of aquifers such as unconfined or leaky aquifers. It can also consider the impact of bounded aquifers such as aquifers with prescribed head or no-flow boundaries.
- This study considered two-dimensional flow. The interpretation techniques can be extended in the future, to three-dimensional flow problems. Three-dimensional flow is more realistic however, it substantially complicates with the problem with additional parameters needed to represent the vertical spatial variability.
- Pumping test data were used in this study to estimate the flow parameters and their statistical spatial structure. Future research can consider the combination of pumping test data with other types of data such as tracer test data which involve the injection of a tracer in one well and the monitoring of its concentration at adjacent wells as a function of time.
- The current study focuses on methods used for the representation of the spatial variability of the flow parameters. Future research could consider the impact of the spatial variability on contaminant transport.

REFERENCES

- Barker, J. A., Herbert R., 1982. Pumping tests in patchy aquifers. *Ground Water*, 20, 150–155.
- Batu, V., 1998. *Aquifer Hydraulics: A Comprehensive Guide to Hydrogeologic Data Analysis*, John Wiley & Sons, New York.
- Bellin, A., Rubin, Y., 2004. On the use of peak concentration arrival times for the inference of hydrogeological parameters. *Water Resources Research*, 40, W07401, doi:10.1029/2003WR002179.
- Bohling, G. C., Zhan, X., Butler, J. J., Zheng, L., 2002. Steady shape analysis of tomographic pumping tests for characterization of aquifer heterogeneities. *Water Resources Research*, 38, 60-1–60-15.
- Bohling, G., 2005. “Introduction to Geostatistics and Variogram Analysis”, <http://gismyanmar.org/geofocus/wp-content/uploads/2013/01/Variograms.pdf>. (accessed August 2013)
- Butler Jr., J. J., 1988. Pumping tests in nonuniform aquifers - The radially symmetric case. *Journal of Hydrology*, 101, 15–30.
- Butler Jr., J. J., Liu W., 1993. Pumping tests in nonuniform aquifers: The radially asymmetric case. *Water Resources Research*, 29, 259–269.
- Butler Jr., J. J., McElwee, C. D., Bohling, G. C., 1999. Pumping tests in networks of multilevel sampling wells: Motivation and methodology. *Water Resources Research*, 35, 3553-3560.

Cooper Jr., H. H., Jacob, C. E., 1946. A generalized graphical method for evaluating formation constants and summarizing well-field history. *American Geophysical Union Transactions*, 27, 526-534.

Copty, N. K., Findikakis, A. N., 2004a. Stochastic analysis of pumping test drawdown data in heterogeneous geologic formations. *Journal of Hydraulic Research*, 42, 59–67.

Copty, N. K., Findikakis, A. N., 2004b. Bayesian identification of the local transmissivity using time-drawdown data from pumping tests. *Water Resources Research*, 40, W12408, doi:10.1029/2004WR003354.

Copty, N. K., Trinchero P., Sanchez-Vila X., 2011. Inferring spatial distribution of the radially integrated transmissivity from pumping tests in heterogeneous confined aquifers. *Water Resources Research*, 47, W05526, doi:10.1029/2010WR009877.

Dagan, G., 1989. *Flow and Transport in Porous Formations*. Springer-Verlag Heidelberg Berlin, New York.

G. Dagan, S.P. Neuman (Eds), 1997. *Subsurface Flow and Transport: A Stochastic Approach*. International Hydrology Series, Cambridge University Press, New York.

Deutsch, C., Journel A., 1992. *GSLIB: Geostatistical Software Library and User's Guide*, Oxford University Press, New York.

Domenico, P. A., Schwartz, F. W., 1998. *Physical and Chemical Hydrogeology*, Wiley, New York.

Elfeki, A. M. M., Uffink, G. J. M., Barends, F. B. J., 1997. *Groundwater Contaminant Transport: Impact of Heterogeneous Characterisation: A New View on Dispersion*. Balkema Publishers, Rotterdam, Netherlands.

Feinerman, E., Dagan, G., and Bresler, E., 1986. Statistical inference of spatial random functions. *Water Resources Research*, 22, 935-942.

Fetter, C. W., 1994. Applied Hydrogeology, Macmillan, New York.

Freeze, R. A., Cherry, J. A., 1977. Groundwater. Prentice-Hall, New Jersey.

Firmani, G., Fiori, A., and Bellin, A., 2006. Three-dimensional numerical analysis of steady state pumping tests in heterogeneous confined aquifers. *Water Resources Research*, 42, W03422, doi:10.1029/2005WR004382.

Gelhar, L. W., 1993. Stochastic Subsurface Hydrology. Prentice-Hall, New Jersey.

Gottlieb, J., Dietrich, P., 1995. Identification of the permeability distribution in soil by hydraulic tomography. *Inverse Problems*, 11, 353-360.

Hantush, M. S., Jacob, C. E., 1955. Non-steady radial flow in an infinite leaky aquifer. *American Geophysical Union Transactions*, 36, 95-100.

Harbaugh, A., Banta E., Hill M., McDonald M., 2000. Modflow-2000: The US Geological Survey modular ground-water model-user guide to modularization concepts and the ground-water flow process. USGS Open-File Report 00-92. Reston, Virginia.

Hoeksema, R. J., Kitanidis, P. K., 1985. Comparison of gaussian conditional mean and kriging estimation in the geostatistical solution of the inverse problem. *Water Resources Research*, 21, 825-836.

Hornberger G.M., Spear, R.C., 1981. An approach to the preliminary analysis of environmental systems. *Journal of Environmental Management*, 12, 7-18.

Huang, H., Hu, B. X., Wen, X. H., Shirley, C., 2004. Stochastic inverse mapping of hydraulic conductivity and sorption partitioning coefficient fields conditioning on nonreactive and reactive tracer test data. *Water Resources Research*, 40, W01506, doi: 10.1029/2003WR002253.

Kemper, K., 2004. Groundwater-from development to management. *Hydrogeology Journal*, 12, 3-5.

Kitanidis, P. K., 1986. Parameter uncertainty in estimation of spatial functions: Bayesian analysis. *Water Resources Research*, 22, 499-507.

Kitanidis, P. K., 1997. *Introduction to Geostatistics: With Applications in Hydrogeology*, Cambridge University Press, New York.

Kruseman, G. P., Ridder, N. A., 1990. *Analysis and Evaluation of Pumping Test Data*. International Institute for Land Reclamation and Improvement, Wageningen, The Netherlands.

Kumar, C. P., 2006. Groundwater Flow Models: An Overview. In Ghosh, N. C., Sharma, K.D. (Eds), *Groundwater Modelling and Management*, Capital Publishing Company, New Delhi, 153-178.

Leven, C., Dietrich, P., 2006. What information can we get from pumping tests?- Comparing pumping test configurations using sensitivity coefficients, *Journal of Hydrology*, 319, 199–215.

Mantoglou, A., Wilson, J. L., 1982. The turning bands method for simulation of random fields using line generation by a spectral method. *Water Resources Research*, 18, 1379-1394.

Meier, P. M., Carrera, J., Sanchez-Vila, X., 1998. An evaluation of Jacob's method for the interpretation of pumping tests in heterogeneous formations, *Water Resources Research*, 34, 1011–1025.

McDonald, M. G., Harbaugh, A. W., 1988. *A Modular Three-Dimensional Finite-Difference Groundwater Flow Model*. US Geological Survey Techniques of Water-Resources Investigations, Book 6, USGS Open-File Report 83-875, Reston, Virginia.

Metropolis, N., Ulam, S., 1949. The Monte Carlo method. *Journal of the American Statistical Association*, 44, 335-341.

Mosegaard, K., Tarantola, A., 1995. Monte Carlo sampling of solutions to inverse problems. *Journal of Geophysical Research*, 100, 12,431-12,447.

Neuman, S. P., Guadagnini, A., Riva M., 2004. Type-curve estimation of statistical heterogeneity. *Water Resources Research*, 40, W04201, doi:10.1029/2003WR002405.

Neuman, S. P., Blattstein, A., Riva, M., Tartakovsky, D. M., Guadagnini, A., Ptak, T., 2007. Type curve interpretation of late-time pumping test data in randomly heterogeneous aquifers. *Water Resources Research*, 43, W10421, doi:10.1029/2007WR005871.

Oliver, D. S., 1993. The influence of nonuniform transmissivity and storativity on drawdown. *Water Resources Research*, 29, 169–178.

Pinder, G. F., Celia, M. A., 2006. *Subsurface Hydrology*. John Wiley & Sons, New York.

Renard, P., 2007. Stochastic hydrogeology: what professionals really need?. *Ground Water*, 45, 531-541.

Riva, M., Guadagnini, A., Bodin, J., Delay, F., 2009. Characterization of the hydrogeological experimental site of Poitiers (France) by stochastic well testing analysis. *Journal of Hydrology*, 369, 154–164.

Rubin, Y., 2003. *Applied Stochastic Hydrogeology*: Oxford University Press. New York.

Rubin, Y., Hubbard, S. S., 2005. *Hydrogeophysics*, Springer, Netherlands.

Sánchez-Vila, X., Meier, P. M., Carrera, J., 1999. Pumping tests in heterogeneous aquifers: An analytical study of what can be obtained from their interpretation using Jacob's method. *Water Resources Research*, 35, 943-952.

Schad, H., Teutsch, G., 1994. Effects of the investigation scale on pumping tests results in heterogeneous porous aquifers, *Journal of Hydrology*, 159, 61–77.

Shiklomanov, I., 1993. World fresh water resources. In Gleick, P. H. (Ed.) *Water in crisis: a guide to the world's fresh water resources*. Oxford University Press, New York.

Slater, L., 2007. Near surface electrical characterization of hydraulic conductivity: From petrophysical properties to aquifer geometries—A review. *Surveys in Geophysics*, 28, 169-197.

Theis, C. V., 1935. The relation between the lowering of the piezometric surface and the rate and duration of discharge of a well using ground water storage. *American Geophysical Union Transactions*, 16, 519–524.

Vandenberg, A., 1977. Series expression for the well function for leaky strip aquifers. *Journal of Hydrology*, 34, 389-394.

Walton, W. C., 1970. *Groundwater Resources Evaluation*, Mc-Graw Hill Book Company, New York.

Yeh, T. C. J., Gutjahr, A. L., Jin, M., 1995. An iterative cokriging-like technique for ground-water flow modeling. *Ground Water*, 33, 33-41.

Yeh, T. C. J., Liu, S., 2000. Hydraulic tomography: Development of a new aquifer test method. *Water Resources Research*, 36, 2095-2105.

Younger, P. L., 2007. *Groundwater in the Environment: An Introduction*. Blackwell Publishing, Oxford.

Zhang, D., 2002. *Stochastic Methods for Flow in Porous Media*, Academic, San Diego, California.

APPENDIX A: COMPUTER CODE FOR THE APPLICATION OF CONTINUOUS DERIVATION METHOD

```

c   Calculates the apparent transmissivity and storativity as a function of time
c   and radial distance using the method of derivatives (Universal Method)   for:
c   CONFINED aquifers (iaquifer=1)
c   *****
implicit double precision (a-h,o-z)
parameter(nreal=1000,ngroup=1,nobs=1,nsim=nreal*ngroup,nstep=220,
& q=2.,h0=20.,iaquifer=1,nwellf=17*1000,iwell=241,jwell=241)
c   iaquifer=1   Confined Aquifers
dimension h(nobs,nstep),s(nobs,nstep),radius(nobs)
dimension time(nstep),tao(nstep),t_ave(nstep)
dimension u(nwellf),wellfunc(nwellf)
dimension trans(nobs,nstep),stor(nobs,nstep),diffus(nobs,nstep)
dimension t(481,481),tlweight(nreal,241)
dimension tmean1(240),tmean2(240),torder(nreal,240)
dimension t_cj(nobs),t_cj2(nobs),s_cj(nobs),s_cj2(nobs)
character filein*10, casenum*2, runnum(nreal)*8
character filein2*10, runsim(nreal)*8
c input/output file names:
open(4,file='dummy',status='old')
open(14,file='hetero1.txt',status='old')
open(5,file='time.txt',status='old')
open(6,file='temp.out',status='unknown')
open(7,file='parameters1.out',status='unknown')
open(8,file='parameters2.out',status='unknown')
open(9,file='parameters3.out',status='unknown')
open(11,file='wellfunc.out',status='unknown')
open(17,file='scatter.out',status='unknown')
open(18,file='cj.out',status='unknown')
open(19,file='sss.out',status='unknown')

```

```

open(3,file='dummy2',status='old')
open(12,file='effect.out',status='unknown')
open(13,file='quartiles.out',status='unknown')
c   Define the distance from observation point to pumping well
do 12 i=1,nobs
if(i.eq.1)radius(i)=0.2
12  continue
c read head data
do 15 j=1,nstep
read(5,*)tmodflow
time(j)=tmodflow/86400.
tao(j)=log10(time(j))
15  continue
do 20 k1=1,ngroup
read(14,'(a2)') casenum
do 22 k2=1,nreal
if(k1.eq.1) read(4,'(a8)') runnum(k2)
filein(1:2)=casenum
filein(3:10)=runnum(k2)
write(*,3)filein
3   format(1x,a10)
c   i=k2+nreal*(k1-1)
open(15,file=filein,status='old')
do 30 j=1,nstep
read(15,4)nt,(h(i,j),i=1,nobs)
4   format(i5,65f12.7)
do 31, i=1,nobs
s(i,j)=h0-h(i,j)
31  continue
30  continue
c     goto 789
c   read the point transmissivity values
if(k1.eq.1) read(3,'(a8)') runsim(k2)

```

```

filein2(1:2)=casenum
filein2(3:10)=runsim(k2)
write(*,3)filein2
open(16,file=filein2,status='old')
do 32 i=1,481
read(16,5)(t(i,j),j=1,481)
5  format(10f9.4)
32  continue
c  calculate the effective transmissivity weighted average of the point transmissivity
values
do 33 ii=1,241
tlweight(k2,ii)=0.
weight=0.0
sumweigh=0.0
dist=float(ii)
do 34 i=iwell-ii,iwell+ii
do 35 j=jwell-ii,jwell+ii
if(i.le.0.or.j.le.0.or.i.gt.481.or.j.gt.481) goto 35
ddd=sqrt((float(i-iwell))**2+(float(j-jwell))**2)
if(ddd.le.dist) then
weight=1
tlweight(k2,ii)=tlweight(k2,ii)+log(t(i,j))*weight
sumweigh=sumweigh+weight
endif
35  continue
34  continue
tlweight(k2,ii)=tlweight(k2,ii)/sumweigh
write(12,6)float(ii),exp(tlweight(k2,ii)),sumweigh
6  format(20f12.4)
33  continue
c *****
c  calculate the flow parameters using
c  Universal method for Confined aquifers (iaquifer=1),

```

```

789   if(iaquifer.eq.1)then
write(*,*)k1,k2
c   calculate the well function (once only)
if(k1.eq.1.and.k2.eq.1)then
call Well(u,wellfunc)
do 320 iw=1,nwellf
write(11,301) iw,u(iw),wellfunc(iw),wellfunc(iw)*exp(u(iw))
320  continue
301  format(i5,3d15.8)
write(*,*)"wellfunction computed"
endif
do 70 i=1,nobs
c   calculate T_cj(i) and S_cj(i) using the Cooper-Jacob method
slope=(s(i,150)-s(i,140))/(tao(150)-tao(140))
t_cj(i)=2.302*2./(4.*3.14159*slope)
abc=s(i,150)*4*3.14159*t_cj(i)/2.302/2.
s_cj(i)=2.25*t_cj(i)*time(150)/radius(i)**2/10**(abc)
slope=(s(i,140)-s(i,130))/(tao(140)-tao(130))
t_cj2(i)=2.302*2./(4.*3.14159*slope)
abc=s(i,140)*4*3.14159*t_cj2(i)/2.302/2.
s_cj2(i)=2.25*t_cj2(i)*time(140)/radius(i)**2/10**(abc)
do 75 j=1,nstep-1
c   initialize solution arrays
diffus(i,j)=-9.
trans(i,j)=-9.
stor(i,j)=-9.
www=0.
c   calculate drawdown rate
ds=(s(i,j+1)-s(i,j))/(tao(j+1)-tao(j))
c   calculate time and drawdown at the center of the time interval
t_ave(j)=0.5*(tao(j+1)+tao(j))
s_ave=0.5*(s(i,j+1)+s(i,j))
u_ave=radius(i)**2*0.0001/4/10**(t_ave(j))

```

```

c   the method is not applicable to very small t because the numerical and Theis solutions
c   are not identical
if(u_ave.gt.100) goto 75
if(ds.ge.0.0000001)then
www=log(10.)*s_ave/ds
if(i.eq.3)write(19,7)i,j,10**(t_ave(j)),ds,www
7   format(2i5,3e15.8)
do 81 k=1,nwellf
x1=wellfunc(k)*exp(u(k))
x2=wellfunc(k+1)*exp(u(k+1))
if(www.le.x1.and.www.gt.x2)      then
c   interpolate
slope=(u(k+1)-u(k))/(x2-x1)
u0=u(k)+slope*(www-x1)
slope=(wellfunc(k+1)-wellfunc(k))/(x2-x1)
well0=wellfunc(k)+slope*(www-x1)
c   calculate diffusivity
diffus(i,j)=radius(i)**2/4./10**(t_ave(j))/u0
c   calculate transmissivity
trans(i,j)=q*well0/4/3.14159/s_ave
c   calculate storativity
stor(i,j)=trans(i,j)/diffus(i,j)
goto 80
endif
81  continue
endif
80  continue
75  continue
70  continue
do 84, i=1,nobs
write(18,11)k1,k2,radius(i),t_cj(i),t_cj2(i),s_cj(i),s_cj2(i)
84  continue
do 85 j=1,nstep-1

```

```

write(7,11)k1,k2,10**(T_ave(j)),
& sqrt(4*(10**T_ave(j))*Trans(1,j)/(1.65*0.0001)),Trans(1,j)
write(8,11)k1,k2,10**(T_ave(j)),
& sqrt(4*(10**T_ave(j))*Trans(1,j)/(1.65*0.0001)),stor(1,j)
write(9,11)k1,k2,10**(T_ave(j)),
& sqrt(4*(10**T_ave(j))*Trans(1,j)/(1.65*0.0001)),diffus(1,j)
85 continue
11 format(2i5,66f16.9)
endif
22 continue
write(7,*)
20 continue
c order the transmissivity estimates to compute mean and upper/lower quartiles
do 169 m1=1,nreal
write(13,170)(tlweight(m1,ii),ii=1,240)
169 continue
c order the weighted transmissivity data
do 166 ii=1,240
do 167 m1=1,nreal
torder(m1,ii)=+999.
do 168 m2=1,nreal
if(m1.eq.1)then
tmean1(ii)=tmean1(ii)+exp(tlweight(m2,ii))/float(nreal)
tmean2(ii)=tmean2(ii)+tlweight(m2,ii)/float(nreal)
endif
if(torder(m1,ii).gt.tlweight(m2,ii)) then
torder(m1,ii)=tlweight(m2,ii)
imin=m2
endif
168 continue
tlweight(imin,ii)=+9999.
167 continue
166 continue

```

```

write(13,170)(torder(100,ii),ii=1,240)
write(13,170)(torder(250,ii),ii=1,240)
write(13,170)(tmean1(ii),ii=1,240)
write(13,170)(tmean2(ii),ii=1,240)
write(13,170)(torder(500,ii),ii=1,240)
write(13,170)(torder(750,ii),ii=1,240)
write(13,170)(torder(900,ii),ii=1,240)
170  format(240f10.4)
999  stop
end

subroutine Well(u,wellfunc)
c   calculates the well function
implicit double precision (a-g,o-z)
parameter (nwellf=17*1000)
dimension u(nwellf),uog(nwellf),func(nwellf),wellfunc(nwellf)
c   define the  $u=r^2S/4tT$  values from  $1e-15$  to  $1e+2$ 
uog(1)=-15
u(1)=10**(uog(1))
do 20 i=2,nwellf
uog(i)=uog(i-1)+0.001
u(i)=10**(uog(i))
20  continue

c   calculate the function (appearing in the integration) for u values from  $1e-15$  to  $1e+2$ 
do 50 i=1,nwellf
func(i)=exp(-u(i))/u(i)
50  continue

c   calculate the well function for u values from  $1e-15$  to  $1e+2$ 
c   or  $1/u$   $1e-02$  to  $1e+15$ 
do 70 i=nwellf,1,-1
if(i.eq.nwellf) goto 70
c   calculate integral using Trapezoid Rule
wellfunc(i)=wellfunc(i+1)+0.5*(func(i)+func(i+1))*(u(i+1)-u(i))
c   calculate integral using Simpson's Rule

```

```
c MUST CORRECT BECAUSE NOT EQUALLY SPACED
c     u_ave=0.5*(u(i+1)+u(i))
c     func_ave=1./u_ave*exp(-u_ave)**2/4./u_ave)
c     wellfunc(i)=wellfunc(i+1)+(func(i)+4.*func_ave+func(i))*(u(i+1)-u(i))/6.
70  continue
return
end
```

APPENDIX B: COMPUTER CODE FOR THE ESTIMATION OF STATISTICAL PARAMETERS

```

c   calculates the integral scale and variance by minimizing the
c   difference between theoretical family of curves and the estimated T vs radius
c   ****

parameter(nreal=1000,ngroup=1,nobs=1,nsim=nreal*ngroup,nstep=220,
& nmax=120,nave=10)
dimension T_est(nreal,nstep),r_est(nreal,nstep)
dimension r_th(240),T_th(41,240),sigma(41)
dimension T_int(nreal,nmax),r_int(nmax)
dimension T_ave(nreal/nave,nmax)
dimension errsum(41,41),r11x(149)
dimension tnew(41,149),t2(41,149)
open(4,file='1.txt',status='old')
open(5,file='parameters1-52',status='old')
open(6,file='rer.txt',status='unknown')
open(7,file='result3-6.txt',status='unknown')
open(8,file='tnew.txt',status='unknown')
c   read estimated transmissivity data
do 5 i=1,nreal
do 10 j=1,nstep-1
read(5,*) k1,k2,time,r_est(i,j),T_est(i,j)
10   continue
5    continue
c   interpolate T_est on equally spaced distance intervals
do 55 i=1,nmax
r_int(i)=float(i)
do 11 k=1,nreal
do 40 j=1,nstep-1
if(r_int(i).lt.r_est(k,j)) then

```

```

T_int(k,i)=T_est(k,1)
goto 11
endif
if(r_est(k,j).le.r_int(i).AND.r_est(k,j+1).ge.r_int(i)) then
T_int(k,i)=T_est(k,j)+((T_est(k,j+1)-T_est(k,j))*
&(r_int(i)-r_est(k,j))/(r_est(k,j+1)-r_est(k,j)))
goto 11
endif
40    continue
11    continue
55    continue
c      Averaging nave T vs r curves
do 65 i=1,nreal/nave
do 75 j=1,nmax
do 85 k=1,nave
T_ave(i,j)=T_ave(i,j)+T_int(nave*(i-1)+k,j)/nave
85    continue
75    continue
65    continue
c    read theoretical family of curves of T/sigma vs r/I
do 70 j=1,240
if(j.eq.1) read(4,*) dummy,(sigma(i),i=1,41)
read(4,*) r_th(j),(T_th(i,j),i=1,41)
70    continue
do 25 ii=1,41
do 26 j=1,149
r11x(j)=r_th(j)/float(ii)
26    continue
do 30 i=1,41
do 50 j=1,nmax
do 60 k=1,239
if((r11x(j)).lt.r_th(1)) then
tnew(i,j)=T_th(i,1)

```

```

goto 50
endif
if((r11x(j)).gt.r_th(240)) then
tnew(i,j)=1
goto 50
endif
if((r11x(j)).ge.r_th(k). AND . (r11x(j)).le.r_th(k+1)) then
t2(i,j)=((r11x(j))-r_th(k))*(T_th(i,k+1)-T_th(i,k))
tnew(i,j)=(t2(i,j)/0.125)+T_th(i,k)
goto 50
end if
60    continue
50    continue
30    continue
do 20 i=1,41
do 15 j=1,nmax
do 33 k=1,nreal/nave
errsum(ii,i)= errsum(ii,i)+(T_ave(k,j)-tnew(i,j))**2
33    continue
15    continue
20    continue
25    continue
do 100 i=1,nreal/nave
write(8,9)(T_ave(k,j),j=1,nmax)
9      format(149f15.7)
100   continue
c     do 90 i=1,41
do 80 ii=1,41
write(7,8)(errsum(ii,i),i=1,41)
8     format(45f15.7)
80    continue
stop
end

```